OXFORD UNIVERSITY PRESS | Cerebral Cortex

Developmental expression patterns of KCC2 and functionally associated molecules in the human brain

Journal:	*Cerebral Cortex*
Manuscript ID:	CerCor-2015-00656.R2
Manuscript Type:	Original Articles
Date Submitted by the Author:	n/a
Complete List of Authors:	Sedmak, Goran; University of Zagreb School of Medicine, Croatian Institute for Brain Research, Departmet of Neuroscience Jovanov-Milošević, Nataša; University of Zagreb School of Medicine, Croatian Institute for Brain Research, Department of Neuroscience Puskarjov, Martin; University of Helsinkki, Department of Biosciences and Neuroscience Center Ulamec, Monika; University of Zagreb School of Medicine, Department of Pathology; Clinical Hospital Center Sisters of Mercy, Department of Pathology Krušlin, Božo; University of Zagreb School of Medicine, Department of Pathology; Clinical Hospital Center Sisters of Mercy, Department of Pathology Kaila, Kai; University of Helsinki, Biosciences; Judas, Milos; University of Zagreb School of Medicine, Croatian Institute for Brain Research, Department of Neuroscience
Keywords:	human brain, cation-chloride cotransporters, SLC12, Na-K ATPase, KCC2

Developmental expression patterns of KCC2 and functionally associated molecules in the human brain

Goran Sedmak[1*], Nataša Jovanov-Milošević[1*], Martin Puskarjov[2*], Monika Ulamec[3], Božo Krušlin[3], Kai Kaila[2], Miloš Judaš[1]

[1]University of Zagreb School of Medicine, Croatian Institute for Brain Research, Šalata 12, 10 000 Zagreb, Croatia

[2]University of Helsinki, Department of Biosciences and Neuroscience Center, Viikinkaari 1, FI-00014 Helsinki, Finland

[3]University of Zagreb School of Medicine, Clinical Hospital Center Sisters of Mercy, Department of Pathology, Vinogradska cesta 29, 10 000 Zagreb, Croatia.

[*]These authors contributed equally to this work

Address correspondence to
Prof. Miloš Judaš, M.D., D.Sc.
University of Zagreb School of Medicine
Croatian Institute for Brain Research
Šalata 12, 10 000 Zagreb, Croatia
Phone: +385 (1) 4596 801
E-mail: mjudas@hiim.hr
and to
Prof. Kai Kaila, PhD
Department of Biosciences and Neuroscience Center
University of Helsinki
Viikinkaari 1,FI-00014 Helsinki, Finland
Phone: +358 40 7256759
E-mail: kai.kaila@helsinki.fi

Abstract

Work on rodents demonstrated that steep up-regulation of KCC2, a neuron-specific Cl^- extruder of cation-chloride cotransporter (CCC) family, commences in supraspinal structures at around birth, leading to establishment of hyperpolarizing GABAergic responses.

We describe spatiotemporal expression profiles of the entire CCC family in human brain. KCC2 mRNA was observed already at 10^{th} postconceptional week (PCW) in amygdala, cerebellum and thalamus. KCC2-immunoreactive (KCC2-ir) neurons were abundant in subplate at 18 PCW. By 25 PCW numerous subplate and cortical plate neurons became KCC2-ir. The mRNA expression profiles of α and β isoforms of Na-K ATPase, which fuels cation-chloride cotransport, as well of tropomyosin receptor kinase B (TrkB), which promotes developmental up-regulation of KCC2, were consistent with data from studies on rodents about their interactions with KCC2.

Thus, in human brain, expression of KCC2 and its functionally-associated proteins begins in early fetal period. Our work facilitates translation of results on CCC functions from animal studies to human and refutes the view that poor efficacy of anticonvulsants in the term human neonate is attributable to lack of KCC2. We propose that perinatally low threshold for activation of Ca^{2+}-dependent protease calpain renders neonates susceptible to down-regulation of KCC2 by traumatic events, such as perinatal hypoxia-ischemia.

Key words: human brain, cation-chloride cotransporters, SLC12, KCC2, KCC3, NKCC1, TrkB, Na-K ATPase, calpain, calpastatin

Introduction

The mechanisms regulating the intracellular Cl^- concentration ($[Cl^-]_i$) are of fundamental importance in major changes that take place in neuronal signaling during brain development, such as the canonical shift of GABAergic transmission from depolarizing to hyperpolarizing which is caused by up-regulation of the neuron-specific K-Cl cotransporter KCC2 (Rivera et al. 1999; Kaila et al. 2014a). In addition to this, cation-chloride cotransporters (CCCs), most notably KCC2, play important roles in the generation, maintenance and plasticity of neuronal connections (Payne et al. 2003; Ben-Ari et al. 2007; Blaesse et al. 2009; Kaila et al. 2014a). Alterations in the function of CCCs have been implicated in several neurological disorders (Blaesse et al. 2009; Kahle et al. 2013; Kaila et al. 2014a). While a considerable amount of data on CCCs have been obtained in work on laboratory rodents (cf. Ben-Ari et al. 2007; Kaila et al. 2014a), there is little information on their developmental expression patterns in the human brain. Novel information of the kind described above has general implications for human developmental neurobiology, and specific implications for the use of neuronal CCCs as drug targets in the neonate (Puskarjov et al. 2014a).

The solute carrier 12 (SLC12) gene family encompassing the CCCs is composed of nine members (*SLC12A1–9),* seven of which (*SLC12A1–7*) encode for molecules that act as Cl^- transporters. Based on their sequence similarity and transport modes, the CCCs are divided into two major functional branches: the Na^+-dependent Na-(K)-Cl cotransporters (NKCC1, NKCC2 and NCC, respectively encoded by *SLC12A2*, *SLC12A1* and *SLC12A3*) and the K-Cl cotransporters (KCC1–4, encoded by *SLC12A4-7*). The free energy for ion transport by CCCs is derived from the electrochemical Na^+ and K^+ transmembrane gradients maintained by the Na-K ATPase, which is intimately co-expressed and co-regulated with the CCCs (Ikeda et al. 2004; Kaila et al. 2014a; 2014b; Khirug et al. 2010; Fujii et al. 2010). In most CNS neurons, the ubiquitously expressed NKCC1 and the neuron-specific KCC2 are responsible for the generation of ionic driving forces of $GABA_A$ and glycine receptor ($GABA_AR$ and GlyR)-mediated responses (Kaila et al. 2014a). Prior to the robust developmental up-regulation of KCC2, which renders $GABA_AR$ currents hyperpolarizing, a high

intracellular Cl^- concentration ($[Cl^-]_i$) and depolarizing responses to GABA are maintained by NKCC1 in immature cortical principal neurons (Ben-Ari et al. 2007; Kaila et al. 2014a).

The available expression data on the SLC12 gene family in the human brain are scarce (cf. Gagnon and Fulvio 2013) and no spatiotemporal CNS expression profile of the entire SLC12 family has been published. In particular, the available human data are inconsistent with regard to KCC2 (Dzhala et al. 2005; Vanhatalo et al. 2005; Aronica et al. 2007; Bayatti et al. 2008; Jansen et al. 2010; Robinson et al. 2010; Hyde et al. 2011). Some studies report KCC2 protein expression not only in the subplate but also in the cortex in the early fetal period (Bayatti et al. 2008; Robinson et al. 2010), while others suggest that it occurs in the forebrain after term birth (Dzhala et al. 2005; Aronica et al. 2007; Jansen et al. 2010).

The neuron-type and region-dependent expression patterns of KCC2 during brain development have been extensively studied in animal models (for review, see Uvarov et al. 2013; Kaila et al. 2014a). In mammals, KCC2 is abundantly expressed in mature central neurons, with very little or no expression in peripheral neurons, neuronal progenitors and non-neuronal cell types, including glia (Blaesse et al. 2009; Gagnon and Di Fulvio 2013; Kaila et al. 2014a; Uvarov et al. 2013). At the subcellular level, KCC2 is expressed in neuronal cell bodies, dendrites, and dendritic spines, but it is excluded from the axon initial segment and the axon proper (Gulyas et al. 2001; Hübner et al. 2001b; Szabadics et al. 2006; Baldi et al. 2010; Fiumelli et al. 2013). Up-regulation of KCC2 expression takes place strictly in parallel with neuronal differentiation, as reflected in the gradual increase in the caudal-to-rostral direction of the CNS (Li et al. 2002; Stein et al. 2004; Wang et al. 2002). In the caudal parts of the rodent CNS, such as the spinal cord and much of the brainstem, perinatal KCC2 expression patterns are comparable to those observed in older animals (Stein et al. 2004; Blaesse et al. 2006; Balakrishnan et al. 2003; Uvarov et al. 2009). In the more rostral regions, such as the hippocampus and the neocortex, robust up-regulation of KCC2 mRNA commences by the time of birth (Balakrishnan et al. 2003; Rivera et al. 1999; Wang et al. 2002; Li et al. 2002; Stein et al. 2004), reaching a plateau around the third postnatal week (Wang et al. 2002; Rivera et al. 1999). In keeping with the general differences in the milestones of CNS development (Erecinska et al. 2004), the timing

of KCC2 up-regulation with regard to birth is not only brain region- but also species-specific. For instance, in the cortex of neonatal rats and mice, GABA is depolarizing while in the guinea pig – a species with precocious neonates – cortical up-regulation of KCC2 takes place before birth and neonatal guinea pig cortical neurons show hyperpolarizing GABAergic responses (Rivera et al. 1999). Regardless of the relatively low levels of cortical KCC2 in newborn mice and rats, robust alterations in synaptic and network functions in the hippocampal CA3 region have been reported in KCC2 knockout mice at embryonic day 18.5 (Khalilov et al. 2011). This strongly indicates that expression of KCC2 is critical for the development and function of cortical neurons in this species already before birth (see also Horn et al. 2010).

The steep increase in KCC2 expression in the rodent cortex during the first postnatal month (Kovacs et al. 2014; Stein et al. 2004; Sun et al. 2013; Takayama and Inoue 2010) is associated with both the maturation of GABAergic hyperpolarizing inhibition (Rivera et al. 1999) and with intense glutamatergic synaptogenesis and spine formation (De Felipe et al. 1997; Juraska 1982; Fiumelli et al. 2013). KCC2 is not only a key molecule for inhibitory signaling, but its expression is also tightly associated with the morphological development and function of cortical dendritic spines in a manner that is independent of its function as an ion transporter (Li et al. 2007; Gauvain et al. 2011; Chamma et al. 2012; Fiumelli et al. 2013; Puskarjov et al. 2014b; Blaesse and Schmidt 2014; Kaila et al. 2014a). *In vivo* overexpression of KCC2 or its transport-inactive construct is sufficient for *de novo* spinogenesis and formation of functional glutamatergic synapses (Fiumelli et al. 2013; Puskarjov et al. 2014b). Indeed, in a variety of non-human species, the developmental expression of KCC2 has been shown to intimately parallel that of synaptophysin (Ludwig et al. 2003; Zhang et al. 2006; Takayama and Inoue 2006; Bayatti et al. 2008), a molecule routinely used as a proxy for density of glutamatergic synapses (Calhoun et al. 1996; Eastwood et al. 2006). KCC2 is thus likely to act as a coordinating factor in the parallel development and plasticity of synaptic inhibition and excitation (Li et al. 2007; Chamma et al. 2012; Blaesse and Schmidt 2014; Kaila et al. 2014a; Puskarjov et al. 2014b). Recently, a KCC2 point variant found in patients with febrile seizures (Puskarjov et al. 2014b) and idiopathic

generalized epilepsy (Kahle et al. 2014) was shown to lead to deficits in both neuronal Cl^- extrusion capacity and the formation of cortical dendritic spines (Puskarjov et al. 2014b).

Multiple factors have been implicated in controlling the transcriptional up-regulation of mammalian KCC2 (Uvarov et al. 2005; 2006; Markkanen et al. 2008; Yeo et al. 2009; Ludwig et al. 2011a; 2011b). Most notably, signaling mediated by TrkB (Aguado et al. 2003; Carmona et al. 2006; Ludwig et al. 2011b). While the major endogenous ligand of TrkB receptors, brain-derived neurotrophic factor (BDNF), is not necessary for the developmental up-regulation of KCC2 (Puskarjov et al. 2015), signaling mediated by these receptors appears nevertheless to be a major driver of *Slc12a5* transcription in immature rodents (cf. Aguado et al. 2003; Ludwig et al. 2011b). Importantly, levels of mRNA encoding KCC2 are decreased in mice lacking TrkB expression (Carmona et al. 2006). Previous studies on the expression of TrkB in the human brain have been performed mostly on postnatal brain tissue (Romanczyk et al. 2002; Webster et al. 2006; Luberg et al. 2010). Interestingly, near adult-level expression of full-length TrkB protein has been reported in the prefrontal cortex of human neonates (Luberg et al. 2010), however, there is paucity in the data regarding the temporal profile of TrkB expression in the fetal human brain.

Down-regulation of KCC2 has been demonstrated to take place following various neuronal insults via activation of Ca^{2+}-dependent mechanisms, typically downstream of TrkB (Kaila et al. 2014b). We and others have shown that activity-dependent down-regulation of transport-active KCC2 at the post-translational level is a direct consequence of cleavage of the C-terminal domain of KCC2 by either of the two CNS calpains (Puskarjov et al. 2012, 2015; Zhou et al. 2012; Chamma et al. 2013; Jantzie et al. 2014; Kaila et al. 2014a). Hypoxic-ischemic encephalopathy is among the major contributors to long term neurological sequelae in term and pre-term infants, with a close correlation between increased cellular Ca^{2+} uptake and subsequent hypoxic-ischemic neuronal damage within ischemic brain regions (Volpe 2008). Calpains are Ca^{2+}-activated non-promiscuous proteases important for many intracellular processes, such as turnover of cytoskeletal proteins and regulatory cleavage of synaptic proteins, and have been widely implicated in synaptic plasticity as well as neurodegeneration (Goll et al. 2003; Liu et al. 2008; Baudry et al. 2013). In the CNS, calpain 1 and

calpain 2 are the main calpain isoforms and are respectively activated by intracellular Ca^{2+} concentrations in the micro- and millimolar range (Goll et al. 2003). Activation of calpains is restricted by calpastatin, an endogenous calpain-specific inhibitor (Blomgren et al. 1999; Goll et al. 2003; Yang et al. 2013). Notably, calpain overexpression and/or overactivation has been demonstrated to take place in the context of hypoxia-ischemia (Ostwald et al. 1993; Blomgren et al. 1999; Rosenkranz et al. 2012), seizures (Sierra-Paredes et al. 1999; Fujikawa 2005; Puskarjov et al. 2015), and epilepsy (Feng et al. 2011; Das et al. 2012; Kaila et al. 2014b). Interestingly, work on non-human animals suggests that the perinatal period is characterized by a high calpain/calpastatin ratio (Li et al. 2009; Blomgren et al. 1989; Blomgren and Karlsson 1989) and, thus, a low threshold for calpain activation (cf. Simonson et al. 1985; Blomgren and Karlsson 1989; Blomgren et al. 1989; Lu et al. 2000). While down-regulation of KCC2 protein has been reported to take place in preterm infants with white matter lesions (Robinson et al. 2010), it is not known whether this may reflect a heightened susceptibility of KCC2 to calpain cleavage during the perinatal period.

Here, we performed a two-tier analysis of CCC expression in the human brain across development. First, we used microarray data to analyze the spatiotemporal patterns of *SLC12A1-9* mRNA expression in the human brain, and we report for the first time the spatiotemporal expression profile of the entire *SLC12* gene family in the human cerebrum, thalamus and cerebellum. Second, we used KCC2 immunohistochemistry to validate the microarray data on KCC2 expression. Importantly, we found that both *SLC12A5* mRNA and KCC2 protein are robustly up-regulated in the human brain by term birth. Moreover, this is associated with functionally compatible developmental expression patterns of the Na-K ATPase, TrkB, and of synaptic markers. Our work also suggests that the poor efficacy of $GABA_AR$ enhancing anticonvulsant drugs in human neonates is not attributable to lack of cortical KCC2 expression, but is more likely related to the high susceptibility of the perinatal human cortex to KCC2 down-regulation by the calpain system.

Materials and Methods

Microarray data analysis

For the analysis of mRNA expression we used our previously published microarray database (Kang et al. 2011) available from the Gene Expression Omnibus (GEO accession GSE 25219, Human Exon 1.0 ST Array). The dataset is composed of 1340 brain tissue samples encompassing the entire human lifespan (age range 5 PCW–82 years) and covering 16 brain regions (for details see Suppl. Table 1, and Kang et al. 2011). Partek Genomic Suite 6.6 (Partek Inc.) was used to normalize data and summarize probe set and transcript clusters. Affymetrix CEL files were imported into Partek Genomic Suite using default Partek settings. Analysis was done on the probe sets designated as 'core' and 'extended' using Partek Genomic Suite 6.6 and R Statistical Software Package (http://www.r-project.org). The analyzed probe sets covered the entire span of the gene. Therefore, in the subsequent analysis all known mRNA isoforms were included and data presented is the average expression of all isoforms. The median of all probesets within one gene was used as the estimate of gene expression. The data is presented as $\log_2$-transformed value of the signal intensity and a gene was considered as expressed when the $\log_2$-transformed expression value in the analyzed sample was ≥ 5.5 (cf. Kang et al. 2011).

Immunohistochemistry

To analyze the developmental expression patterns of KCC2 in the human brain at protein level, we took advantage of the extensive Zagreb Collection of human brains and indirect immunohistochemistry (Kostovic et al. 1991; Judas et al. 2011). Nissl stainings were performed on adjacent histological sections for delineation of developmental layers and cytoarchitectonic boundaries and cellular compartments. In total 17 human postmortem brains were analyzed, including 13 fetal brains (age range: 16–40 PCW), 2 infant brains (aged 3 and 13 months), one child brain (aged 6.5 years) and one adult brain (aged 51 years). Brains were collected at the pathology department of the

University of Zagreb School of Medicine. Fetal brain specimens were obtained either from medically-indicated or spontaneous abortions or subsequent to the death of prematurely born neonates. Fetal ages were determined on the basis of crown-rump lengths and pregnancy records, and expressed as PCW. All postnatal brain specimens were collected during autopsies according to the protocol approved by the Institutional Review Board with the parental or next of kin consent. The brains analyzed in this study did not exhibit microscopic or macroscopic signs of pathological changes.

Whole brains (postmortem delay 6–24 hrs, for details see Suppl. Table 2) were immersion-fixed using 4% paraformaldehyde in 0.1 M phosphate buffer (pH 7.4). Subsequently, tissue blocks were either frozen or embedded in paraffin and cut in coronal plane at a thickness of 20 µm (paraffin-embedded tissue) or 100 µm (frozen tissue). Immunohistochemistry was performed according to standard protocols (Hsu et al. 1981). Following dewaxing and rehydration in PBS, antigen retrieval of deparaffinized sections was achieved by microwave heating on 95°C/30 min in citrate buffer saline (pH 6). Thereafter, all sections were pre-treated in 0.3% H_20_2 in a 3:1 mixture of methanol and distilled water for quenching of endogenous peroxidase and washed for 10 min in PBS. To prevent non-specific background staining sections were immersed in blocking solution (3% bovine serum albumin and 0.5% Triton X-100 in PBS; all from Sigma) for 2 hrs at room temperature (RT) and then incubated overnight at 4°C with a polyclonal rabbit-anti-KCC2 C-terminal primary antibody (1:2000) (Ludwig et al. 2003). Following a 1 h wash in PBS, a biotinylated anti-rabbit secondary antibody (Vectastain ABC kit) was applied (1:200 in blocking solution) for 1h at RT. The sections were then washed for 1 h and immersed in streptavidin/peroxidase complex (1:500 in PBS) (Vectastain ABC kit) for 1h at RT. The peroxidase activity was visualized using Ni-3,3-diaminobenzidine (Sigma). Sections were then dehydrated in graded series of alcohol, cleared in xylene and cover-slipped using Histomount (National Diagnostics). Negative controls were included in all experiments: by either replacing the primary antibody with blocking solution or preimmune goat or horse serum or by omitting secondary antibody or replacing it with anti-mouse secondary antibody. No immunolabeling was detected in these control sections. Qualitative analysis of the sections was performed using an Olympus Provis AX70 upright microscope (Olympus), and sections were digitized using a

NanoZoomer 2.0-RS digital slide scanner (Hamamatsu Photonics) at 400x magnification. Selected images were exported from virtual slides using NDP.view2 software (Hamamatsu Photonics) and processed using Adobe Photoshop CS5 (Adobe Systems).

Results

Spatio-temporal expression patterns of SLC12A1-9 mRNA in the human brain

Microarray mRNA expression data of the nine known members of the *SLC12A* family was analyzed in 16 human brain regions at 13 different developmental periods (Fig. 1, Suppl. Fig. 1, Suppl. Table 1). Five members (*SLC12A1* [encoding for NKCC2], *SLC12A3* [NCC], *SLC12A7* [KCC4], *SLC12A8* [CCC9], and *SLC12A9* [CIP1]) of the *SLC12A* family were not detected in any of the brain regions analyzed at any developmental period (Suppl. Fig. 1; Suppl. Tables 3–7). Two (*SLC12A2* [NKCC1] and *SLC12A6* [KCC3]) were observed in all regions at all periods (Fig. 1; Suppl. Tables 8 and 9) and displayed an opposite pattern of mRNA expression. *SLC12A2* exhibited lower levels during the prenatal period (10 PCW–birth) with an increase in expression during the postnatal period (birth–90 years). *SLC12A6* exhibited higher levels during the prenatal period with a decrease in expression during the postnatal period. The remaining two CCCs genes, *SLC12A4* [KCC1] and *SLC12A5* [KCC2], displayed a restricted spatio-temporal pattern of transcript expression. *SLC12A4* was limited to the cerebellar cortex, hippocampus, striatum and the mediodorsal nucleus of the thalamus (Fig. 1, Suppl. Table 10). *SLC12A4* was first observed in the cerebellar cortex between 10-13 PCW, followed by expression in other regions between 24 PCW and birth (Fig. 1). In contrast, *SLC12A5* was detected in all regions with a prominent developmental up-regulation across the brain regions examined (Fig. 1, Suppl. Table 11). The amygdala, cerebellar cortex and the mediodorsal nucleus of the thalamus were the first regions where *SLC12A5* mRNA was observed (at 10–13 PCW), followed by hippocampus, striatum and the neocortex (at 16–19 PCW; Fig. 1). By 19–24 PCW *SLC12A5* mRNA was present in the majority of neocortical regions, with one region (primary motor cortex) expressing KCC2 at an earlier period (16–19 PCW) and two regions (dorsolateral frontal cortex, and primary visual cortex) somewhat later (24 PCW–birth). A significant level of mRNA encoding KCC2 was present during the last trimester of pregnancy in all analyzed neocortical regions and an adult-like level was reached between birth and the sixth postnatal month (Fig. 1).

Expression patterns of KCC2 protein in the developing human brain

Following the analysis of microarray mRNA expression data, we studied the developmental expression patterns of KCC2 protein in the human brain. At 16 PCW, no KCC2-immunoreactive (KCC2-ir) neurons were observed either in the cortical plate or the subplate (Fig. 2*A, F*). We first identified KCC2-ir neurons in the subplate at 18 PCW, with only few scattered KCC2-ir neurons in the cortical plate. These data are in close agreement with a previous immunohistochemical study reporting that in the developing neocortex, KCC2 is first expressed in the inner subplate by 16 PCW (Bayatti et al. 2008). From 25 PCW onwards, KCC2-ir neurons were readily observed in both the cortical plate and the subplate (Fig. 2*B–D*, *G–I;* Suppl. Fig. 2). In the adult brain, KCC2-ir neurons were present in all neocortical layers as well as in the subcortical (gyral) white matter (Fig. 2*E*, *J*). In the cingulate cortex at 20 PCW, KCC2-ir neurons were present in the subplate but not in the cortical plate, where they appeared at 25 PCW (Suppl. Fig. 3*A*). At that age, KCC2-ir was present in somata and proximal dendrites of cortical plate neurons (Suppl. Fig. 3*A*), as well as in subplate neurons (Suppl. Fig. 3*E*); and this pattern of expression remained similar until birth (Suppl. Fig. 3*B*, *F*). By the time of birth, strong KCC2-ir was present in somata and proximal dendrites of neurons of all cortical layers (Suppl. Fig. 3*C*, *D*) as well as in subplate neurons (Suppl. Fig. 3*G*) which transform, after first year of life, into interstitial neurons of the subcortical white matter (Suppl. Fig. 3*H*).

In the hippocampus and the entorhinal cortex, KCC2-ir neurons were present already at 25 PCW which, for these regions, was the earliest age analyzed. KCC2-ir neurons with clearly stained somata and proximal dendrites could be observed in the hippocampus and entorhinal cortex from 25 PCW onwards (Fig. 3*A–H*). Strong KCC2-ir of somata and proximal dendrites was also observed in thalamic neurons starting at 22 PCW (Suppl. Fig. 4). Strong KCC2 staining was noted in globus pallidus neurons already at 22 PCW (Suppl. Fig. 5*A*), and this was the region with the highest level of KCC2-ir throughout development (Suppl. Fig. 5*B*, *C*). This raises the interesting possibility that the high immunoreactivity is attributable to KCC2 located in the spines of medium spiny interneurons (cf.

Gulyas et al. 2001). Qualitatively similar, but less pronounced KCC2-ir staining of somata and proximal dendrites was also observed in neurons of claustrum (Suppl. Fig. 5*D*), nucleus caudatus (Suppl. Fig. 5*E*) and putamen (Suppl. Fig. 5*F*).

Developmental expression of TrkB mRNA in the human brain

With regard to the likely role of TrkB in the up-regulation of KCC2 in the human fetal brain, we analyzed the expression patterns of *NTRK2* transcripts encoding for TrkB in the same brain regions as for *SLC12A5*. Strikingly, prenatal up-regulation of *NTRK2*, reaching an adult-like level around birth, was observed in all brain regions investigated (Fig. 4, Suppl. Table 12). A temporal expression profile similar to that of *SLC12A5* was particularly evident in the neocortex and the hippocampus (Fig. 4).

Spatio-temporal expression patterns of Na-K ATPase α and β subunit mRNA in the human brain

The expression level of the Na-K ATPase subunits may pose as a limiting factor for the Cl^--transport function of CCCs (see Introduction). Therefore, we analyzed the spatiotemporal mRNA expression data of the Na-K ATPase α1-4 (*ATP1A1-4*) and β1-4 (*ATP1B1-4*) in the same regions and developmental stages as for the genes encoding for the SLC12 family members. Two of the subunit genes (*ATP1A4* and *ATP1B4*) were not expressed in any of the brain regions analyzed at any developmental period (Figs.5 and 6; Suppl. Tables 16 and 20). Expression of the α4 subunit is largely restricted to the testis in humans and rats (Shamraj and Lingrel 1994). In contrast, *ATP1A1-3* (Fig. 5; Suppl. Tables 13-15) and *ATP1B1-3* (Fig. 6; Suppl. Tables 17-19) mRNA were observed in all analyzed regions at all periods. Expression of *ATP1A2* became significant in all analyzed regions by 16-19 PCW (Fig. 5; Suppl. Table 14) and, together with *ATP1B1-2* (Fig. 6; Suppl. Tables 17-18), underwent robust developmental up-regulation, similar to that of *SLC12A5* (Fig 1; Suppl. Table 11), reaching adult-like expression levels in all studied brain regions around birth. *ATP1A3* mRNA was at low but significant levels at all prenatal periods in all brain regions, except in the striatum (non-

significant at 24 PCW–birth), with postnatal decrease in all analyzed brain regions except mediodorsal nucleus of thalamus (Fig. 5; Suppl. Table 15). The above data suggest that the expression of *neither* α or β subunits of the Na-K ATPase is likely to be a limiting factor for the functionality of secondary-active Cl^- transporters in the developing human brain.

Expression of synaptophysin and PSD-95 mRNA parallel up-regulation of KCC2 in the human brain

While a previous immunohistochemical study demonstrated expression of both KCC2 and synaptophysin as early as 16 PCW in the fetal human neocortex (Bayatti et al. 2008), the developmental relationship between synaptophysin and KCC2, observed in experimental animals, has not been investigated in the human brain. To shed light on this we analyzed the microarray mRNA expression data of *SYP* in the same brain regions and developmental periods as above for *SLC12A5*. *SYP* was significantly expressed in all of the 16 brain regions studied starting from 10 PCW and underwent progressive up-regulation, temporally paralleling that of *SLC12A5*, and reaching adult-like levels around birth in all investigated brain regions (Fig. 7; Suppl. Table 21). As synaptophysin is expressed presynaptically, we also investigated the spatiotemporal mRNA expression profiles of the major postsynaptic density protein PSD-95 (encoded in humans by *DLG4*). In line with the data obtained for *SYP*, *DLG4* exhibited high levels of expression in all brain regions analyzed with significant prenatal up-regulation by the time of birth in all regions investigated (Fig 7: Suppl. Table 22). One exception here was the cerebellar cortex, where a constantly high expression level of *DLG4* was observed.

Together these data support the hypothesis that, akin to observations made in animal models (Ludwig et al. 2003; Takayama and Inoue 2006; Zhang et al. 2006; Fiumelli et al. 2013; Kaila et al. 2014a), up-regulation of KCC2 gene expression spatiotemporally coincides with an intense period of synaptogenesis also in humans. Indeed, the most intense phase of synaptogenesis in humans, or the

brain growth spurt, is observed between the third trimester of pregnancy and the first few years of life (Huttenlocher et al. 1982; Huttenlocher and Dabholkar 1997; Petanjek et al. 2011).

Inverse relationship of calpain and calpastatin mRNA levels in the perinatal human brain

Studies performed in rodents and rabbits have demonstrated that a salient feature of the immature brain is a higher proteolytic potential of the calpain system when compared to later stages in life (Simonson et al. 1985; Blomgren and Karlsson 1989; Blomgren et al. 1989; Lu et al. 2000). This effect is likely to be attributable to the fact that the highest calpain to calpastatin ratio is observed before and around birth in these experimental animals (Li et al. 2009; Blomgren et al. 1989; Blomgren and Karlsson 1989). To investigate whether this is true also in humans, we analyzed in the same brain regions as in those above for *SLC12A5* the spatiotemporal expression patterns of mRNA encoding for the large subunits of calpain 1 and 2 (*CAPN1* and *CAPN2*, respectively), the small regulatory subunit (*CAPNS1*) common to both calpains, and mRNA encoding for the endogenous calpain inhibitor calpastatin (*CAST*). Strikingly, in the majority of brain regions analyzed, most notably in neocortical areas, we observed a large pre to perinatal trough in the developmental expression profile of *CAST* that was paralleled by a developmental peak in the expression of *CAPN1* (Fig. 8; Suppl. Table 23). In the neocortex, expression of both *CAPN1* and *CAPN2* significantly exceeded that of *CAST* throughout pregnancy and until the second half of the first year of life, with the highest calpain to calpastatin mRNA ratio during the last trimester (Fig. 8; Suppl. Tables 23-25). The expression of *CAPNS1* encoding for the small regulatory unit of calpain 1 and 2 was high throughout life (Fig. 8; Suppl. Table 26), and its expression is thus unlikely to act as a limiting factor for calpain activity at any given developmental period.

The above human data are in line with observations made in experimental animals that the threshold for activation of CNS calpains is likely to be lowest during late pregnancy and early postnatal life. More specifically, it indicates that the immature brain is particularly susceptible to calpain-mediated down-regulation of KCC2 under conditions of neuronal damage. This finding

provides a novel point of vantage into the poor efficacy of GABA-enhancing anticonvulsant in neonates with hypoxic-ischemic encephalopathy.

Discussion

This is the first study on the spatiotemporal expression of the entire SLC12 family across human CNS development (see Introduction). In particular, this kind of data are needed on KCC2 which is of unique importance because of its critical roles in the development of both inhibitory and excitatory signaling, and as a potential novel drug target (Gagnon et al. 2013; Löscher et al. 2013b; Kaila et al. 2014a; Puskarjov et al. 2014a). The present data provide the mRNA expression profiles of *SLC12A1-9* in 16 brain regions (11 neocortical areas, hippocampus, amygdala, mediodorsal nucleus of thalamus, and cerebellar cortex) from 10 PCW to 82 years of age.

Our microarray and immunohistochemical data indicate that prominent up-regulation of KCC2 takes place in the human cortex already *in utero*, in contrast to the largely postnatal expression of KCC2 in mice and rats. These data corroborate previously published results linking prenatal up-regulation of *SLC12A5* mRNA with salient changes in the properties of human EEG (Vanhatalo et al. 2005). The cortical EEG of neonatal rats and preterm infants is discontinuous and dominated by discrete network events (Khazipov and Luhmann 2006; Vanhatalo and Kaila 2006). In humans, such events disappear around the time of birth (Vanhatalo et al. 2005), whereas in rats they persist until the second postnatal week (Leinekugel et al. 2002). Thus, in both species, the abolishment of the discrete network events closely parallels the developmental increase in cortical KCC2 (Rivera et al. 1999; Vanhatalo et al. 2005).

Notably, the expression profiles of genes encoding key molecules associated with functional expression of KCC2 (especially the Na-K ATPase) are consistent with the above conclusion. In line with the multifunctional role of human KCC2 in GABAergic signaling and spinogenesis (Kaila et al. 2014a; Puskarjov et al. 2014b), the spatiotemporal expression profiles of *SYP and DLG4* mRNA,

respectively encoding for the synaptic markers synaptophysin and PSD-95, were highly similar to that of KCC2.

Expression patterns of KCC2 in the fetal human brain

The available data on KCC2 expression in the human brain are scarce and inconsistent (Dzhala et al. 2005; Vanhatalo et al. 2005; Aronica et al. 2007; Bayatti et al. 2008; Jansen et al. 2010; Robinson et al. 2010; Hyde et al. 2011). The above studies focused either on a few time points or a single brain region and no systematic analysis of KCC2 protein or mRNA expression has been done. The first study to analyze expression in human brain tissue of the two CCCs critical for neuronal function, NKCC1 and KCC2, was done in the context of pathomechanisms that might underlie neonatal seizures in the perinatal human brain (Dzhala et al. 2005). The authors of this study suggested that the perinatal cerebral cortex of both rodents and humans is characterized by high NKCC1 and negligible levels of KCC2 protein, with gradual down-regulation of NKCC1 and up-regulation of KCC2 during the early postnatal period, the latter reaching adult-like levels after the first year of life (Dzhala et al. 2005; see also Jansen et al. 2010). Findings of that study are often cited in support for the view that the KCC2 expression is low in brains of both preterm and term infants and that it justifies the treatment of neonatal seizures with NKCC1 acting agents, such as bumetanide (cf. Pressler et al. 2015; see also Puskarjov et al. 2014a).

In contrast to the above study, we found that KCC2 expression in the human neocortex begins already during the midfetal period and reaches adult-like levels during the first six months of postnatal life. With respect to human neocortical anlage, we found that the KCC2 expression becomes well established between 18 and 25 PCW. This is in agreement with previous findings of KCC2 expression in the human subplate at 16 PCW (Bayatti et al. 2008) and in the cortical plate at 20 PCW (Robinson et al. 2010; Hyde et al. 2011). Our findings are also in agreement with the general differences in the milestones of neuronal development *vs.* time of birth, where neonate rats and mice are known to

achieve a developmental state of the cortex which roughly corresponds to the start of the third trimester of gestation in the human fetus (cf. Clancy et al. 2001; Erecinska et al. 2004).

The earlier expression of KCC2 in the subplate (18 PCW) than in the cortical plate (25 PCW) probably reflects the fact that subplate neurons are generated earlier and are more mature than neurons of the cortical plate (Hoerder-Suabedissen and Molnar 2015; Kanold and Luhmann 2010; Kostovic and Rakic 1990; Mrzljak et al. 1988; 1990; 1992), and that the subplate represents the major site of synaptogenesis in the human midfetal cerebral wall (Molliver et al. 1973). Between 15 and 24 PCW, the subplate serves as a waiting compartment for cortical afferent fibers which establish numerous temporary synapses with subplate neurons (Kostovic and Rakic 1990; Allendoerfer and Shatz 2003; Kostovic and Judas 2002; 2006; 2007). During the same period, future cortical plate neurons are still young postmitotic neurons which migrate through intermediate and subplate zone towards their final destination in the cortical plate, At 23 to 24 PCW, when most migratory neurons settle in the cortical plate, afferent fibers begin to relocate from the subplate into the cortical plate, which coincides with the onset of intense inside-out synaptogenesis within the cortical plate (Molliver et al. 1973; Kostovic and Rakic 1990). Notably, subplate ablation prevents the developmental up-regulation of KCC2 in cortical layer 4, the main target of thalamocortical axons and subplate neurons (Kanold and Shatz 2006). Our present data suggests that KCC2 expression closely follows the pattern of neuronal differentiation, synaptogenesis and ingrowth of afferent fibers in the subplate and cortical plate during human brain development. Similar findings were reported in rodent cortical neurons where up-regulation of KCC2 expression was demonstrated to take place in parallel with synaptogenesis (Gulyas et al. 2001; Ludwig et al. 2003; Zhang et al. 2006; Takayama and Inoue 2006; see also Fiumelli et al. 2013). Notably, in addition to its role as a K-Cl cotransporter, KCC2 is also critical for the formation and function of cortical dendritic spines in a manner that is independent of its ion transport function (Li et al. 2007; Chamma et al. 2012; Fiumelli et al. 2013; Blaesse and Schmidt 2014; Kaila et al. 2014a; Puskarjov et al. 2014b). Thus, developmental up-regulation of KCC2 is likely to coordinate the development of the major inhibitory and excitatory synaptic signaling systems.

Presently, we observed that in addition to the robust up-regulation of KCC2 expression *in utero*, levels of mRNA encoding for KCC2 continue to increase postnatally during the first 6 months of life (Figs. 1,7-9). Similarly, work on the developing rodent cortex has demonstrated that after the time point when no further increase in Cl^- extrusion capacity is observed in cortical principal neurons (Khirug et al. 2005) further up-regulation in the level of KCC2 protein takes place for up to two weeks thereafter (Sun et al. 2013; Uvarov et al. 2006). This suggests either a high safety factor for maintaining hyperpolarizing GABAergic responses in mature mammalian cortical principal neurons (see Diamond 2002; Puskarjov et al. 2014a); or that the further increase in KCC2 protein serves to facilitate the ion transport-independent functions of KCC2 in synaptogenesis. These two scenarios are mutually non-exclusive, and the latter is consistent with the notion that the peak synaptogenic period in humans takes place during infancy/early childhood (Huttenlocher and Dabholkar 1997; Petanjek et al. 2011) and in the rodent cortex after the ontogenetic shift to hyperpolarizing $GABA_AR$ signaling (De Felipe et al. 1997; Fiumelli et al. 2013; Juraska 1982). Notably, immature rodent hippocampal neurons have the capacity to optimize their use of the available KCC2 levels via increased membrane retention/expression of KCC2 in response to enhanced levels of network activity (Khirug et al. 2010; Bos et al. 2013), an effect that is dependent on BDNF-TrkB signaling (Khirug et al. 2010; Puskarjov et al. 2015).

We also report that robust increase in Na-K ATPase α2 and β2 (and to lesser extent also α1 and β1) mRNA takes place in parallel with up-regulation of KCC2 in the human brain by term birth. Interestingly, recent work on rodent brain Na-K ATPase suggests that to form an active enzyme α1 and α2 subunits assemble preferentially with β1 and β2 subunits, respectively (Tokhtaeva et al. 2012). The α1: β1 and α2:β2 mRNA level stoichiometry apparent in the present data supports the idea that this could be the case also for the human brain Na-K ATPase. Because the energy for Cl^- transport by CCCs depends on the plasmalemmal K^+ and Na^+ gradients, it is interesting that the catalytic α subunits of the Na-K ATPase have been shown to be functionally co-regulated and even to structurally interact with CCCs, including KCC2 (Ikeda et al. 2004; Khirug et al. 2010) and KCC3 (Fujii et al. 2008; 2010; Fujita et al. 2012). Furthermore, analogous interactions between KCC4 and the H-K ATPase (Fujii et

al. 2009) suggest that K-Cl cotransporters form 'ion transport metabolons' (Kaila et al. 2014b) with P-type ATPases. These metabolons may also include ATP-generating molecules, such as the brain type creatine kinase (Inoue et al. 2006; Salin-Cantegrel et al. 2008). Accordingly, transient enhancement in the efficacy of neuronal Cl^- extrusion of immature pyramidal neurons in response to epileptiform activity (Khirug et al. 2010; Puskarjov et al. 2015) is paralleled by increased cell surface expression of both KCC2 and the α2 subunit of the Na-K ATPase (Khirug et al. 2010), and there is indication that this subunit directly interacts with transport-functional KCC2 and is necessary for neuronal Cl^- extrusion (Ikeda et al. 2004). Interestingly, this kind of functional up-regulation of KCC2 depends on the activation of TrkB (add here the refs Khirug et al. 2010; Puskarjov et al. 2015), the receptor of BDNF and NT4 (Park and Poo, 2013).

Notably, we and others have shown that KCC2 is substrate of the Ca^{2+}-dependent protease calpain (Puskarjov et al. 2012, 2015; Zhou et al. 2012; Chamma et al. 2013; Jantzie et al. 2014). This is important as the present study indicates that, as in other mammals (Li et al. 2009; Blomgren et al. 1989; Blomgren and Karlsson 1989), the perinatal period in humans is characterized by a high calpain/calpastatin ratio. It appears that a high proteolytic potential of the calpain system is likely to be one of the hallmarks of the developing, and especially, perinatal mammalian brain. Indeed, during this developmental period calpains have been implicated in maintaining a high rate of synaptic turnover (Lu et al. 2000) in a neuronal activity-dependent Hebbian manner (cf. Lynch and Baudry 1984; Amini et al. 2013). From a clinical perspective, the present work indicates that, in parallel with an apparently smaller safety factor for KCC2 expression (see above), neonates, as compared to older infants and adults, may have a significantly lower threshold for calpain activation (cf. Simonson et al. 1985; Blomgren and Karlsson 1989; Blomgren et al. 1989; Lu et al. 2000) and thus higher susceptibility to calpain-mediated cleavage and functional down-regulation of KCC2 in response to hypoxic-ischemic insults and seizures (Robinson et al. 2010; Puskarjov et al. 2012, 2015; Chamma et al. 2013; Jantzie et al. 2014; see also Ostwald et al. 1993; Blomgren et al. 1999; Kawamura et al. 2005; Rosenkranz et al. 2012; Andres et al. 2013).

NKCC1 mRNA does not exhibit postnatal down-regulation in the human brain

While some studies suggest that NKCC1 expression undergoes postnatal down-regulation (Plotkin et al. 1997; Hübner et al. 2001a; Shimizu-Okabe et al. 2002; Yamada et al. 2004; Dzhala et al. 2005; Liu and Wong-Riley 2012) other studies indicate a postnatal up-regulation of NKCC1 in the CNS during development in rodents (Clayton et al. 1998; Yan et al. 2001; Mikawa et al. 2002) and humans (Hyde et al. 2011; Morita et al. 2014). NKCC1 undergoes alternative mRNA splicing which results in two variants, NKCC1a and NKCC1b (Randall et al. 1997; Vibat et al. 2001; Morita et al. 2014). NKCC1b is highly expressed in the adult brain and constitutes up to ~80% of the total NKCC1 transcript in the human CNS (Vibat et al. 2001). NKCC1 has been suggested to undergo a global down-regulation during development in the rat and human brain (Plotkin et al. 1997; Dzhala et al. 2005). However, this notion is confounded by the use of antibodies and probes insensitive to NKCC1b (cf. Puskarjov et al. 2014a). In line with this, studies based on NKCC1b-compatible mRNA probes and antibodies have demonstrated an absence of developmental down-regulation of NKCC1 in the CNS of rodents and humans (Clayton et al. 1998; Sun and Murali 1999; Yan et al. 2001; Marty et al. 2002; Mikawa et al. 2002; Wang et al. 2002; Hyde et al. 2011; Morita et al. 2014).

Indeed, on the basis of microarray data analysis with probes spanning both major human NKCC1 splice variants NKCC1a and NKCC1b (Vibat et al. 2001; Morita et al. 2014) we found that NKCC1 expression in all of the examined human brain regions undergoes developmental up-regulation. This is in agreement with previously published data on the expression of NKCC1 transcripts in the human hippocampus and prefrontal cortex (Hyde et al. 2011; Morita et al. 2014). This kind of a progressive up-regulation of NKCC1 does not conflict, as might be thought at first sight, with what is known about the development of GABAergic transmission. The extremely high input resistance (R_{in}) of neonatal neurons implies that conductive 'loads' of Cl^- must be very low (see Kaila et al. 2014a). Therefore, a density of plasmalemmal NKCC1 that is sufficient to maintain actions of GABA depolarizing in immature neurons might be functionally barely observable in mature neurons with their much lower R_{in}. Moreover, there is evidence for structural and functional heterogeneity of plasmalemmal NKCC1 expression in adult neurons. The axon initial segment, a

compartment expressing NKCC1 but lacking KCC2, has been shown to be important for maintaining depolarizing (Szabadics et al. 2006; Khirug et al. 2008) but probably functionally inhibitory responses (Kaila et al. 2014a) to GABA in mature cortical principal neurons. Interestingly, NKCC1b, in contrast to NKCC1a, lacks the domain encoded by exon 21, which contains a di-leucine motif that has been implicated in the basolateral vs. apical targeting of NKCC1 in polarized epithelial cells (Kaila et al. 2014a). However, further work is needed to establish the subcellular localization of the NKCC1 splice variants in neurons.

Conclusions

To sum up, our present work describes the developmental patterns of CCCs in the human brain from the fetal stage to senescence. To our knowledge this is the first systematic account of the spatiotemporal expression patterns of the entire SLC12 gene family and also of the genes encoding the α and β subunits of the Na-K ATPase in the human brain. This kind of information is crucial for attempts to translate the extensive amount of information gained from work on the wide spectrum of CCC functions in the developing and mature rodent brain (Ben-Ari et al. 2007; Blaesse et al. 2009; Kaila et al. 2014a) to humans. A point worth of emphasis is that CCCs are gaining an increasing amount of interest as potential drug targets (Gagnon et al. 2013; Töllner et al. 2014), especially with regard to the design of novel anticonvulsant drugs (Löscher et al. 2013b; 2013a). In this context, our data on the fetal onset of KCC2 expression in human supraspinal brain structures (see also Vanhatalo et al. 2005; Bayatti et al. 2008; Robinson et al. 2010; Hyde et al. 2011) refute the view (cf. Dzhala et al. 2005) that the poor efficacy of anticonvulsants in the term human neonate is attributable to a lack of KCC2.

Acknowledgements

This work was supported by the Croatian Science Foundation (grant no. 09.01/414 to MJ) and ERA-NET NEURON II CIPRESS (Academy of Finland to KK) and the Jane and Aatos Erkko Foundation (to KK). Authors gratefully acknowledge the technical assistance of Danica Budinšćak, Božica Popović, Maja Horvat and Ana Jagušt.

Figure legends

Fig. 1. Spatiotemporal expression patterns of *SLC12A family* in the human brain.

The microarray expression data were analyzed for all 9 members of the SLC12 family in 16 brain regions and at 13 different developmental periods (see Suppl. Table 1). Five CCCs (*SLC12A1* [encoding NKCC2], *SLC12A3* [NCC], *SLC12A7* [KCC4], *SLC12A9* [CIP1], *SLC12A8* [CCC9]) were not expressed in the human brain in any region or at any period (Suppl. Fig. 1). Remaining four CCCs (*SLC12A2* [NKCC1], *SLC12A4-6* [KCC1-3]) exhibited diverse spatiotemporal patterns of expression. NKCC1 and KCC3 were expressed in all regions at all periods, while KCC1 and KCC2 had specific patterns of expression (for details see text). Yellow line represents border between expressed (right) and unexpressed (left) samples. Note that in the majority of neocortical regions the onset of KCC2 expression occurs between 19 and 24 PCW.

Fig. 2. Developmental expression pattern of KCC2 immunoreactivity in the neocortex.

At 16 PCW no KCC2-immunoreactive (KCC2-ir) neurons were observed either in cortical plate (A) or subplate (F). KCC2-ir was present in the neocortex from 25 PCW onwards in both the cortical plate (B) and the subplate (G). KCC2-ir neurons at 33 PCW (C, H), 40 PCW (D, I) and 51 years (E, J). KCC2-ir was also present in the adult subcortical white matter interstitial neurons (H). Note the difference between KCC2-ir neuron (arrow in B) and staining artefact (asterisk in B). Bar = 100 μm.

Fig. 3. Developmental expression pattern of KCC2 immunoreactivity in the hippocampus and the entorhinal cortex.

KCC2-ir neurons were observed in the hippocampus (stratum pyramidale) and the entorhinal cortex (layer 3-5) at 25 PCW (A, E), 33 PCW (B, F), 40 PCW (C, G) and 13 months (D, H). Bar = 100 μm.

Fig. 4. Spatiotemporal expression patterns of *NTRK2* in the human brain.

The microarray expression data were analyzed for *NTRK2* (encoding TrkB) in 16 brain regions and at 13 different developmental periods (see Suppl. Table 1). *NTRK2* is expressed in all examined regions from 10 PCW. Note that expression pattern of *NTRK2* follows up-regulation of KCC2 expression in the neocortex.

Fig 5. Spatiotemporal expression patterns of *ATP1A1-4* in the human brain.

The microarray expression data were analyzed for all 4 ATP1A (encoding Na-K ATPase α subunits 1-4) family members in 16 brain regions and at 13 different developmental periods (see Suppl. Table 1). Three members of the family (*ATP1A1-3*) are expressed in the human brain, while *ATP1A4* is not expressed in the human brain at any period. *ATP1A1* starts to be expressed from 10 PCW throughout entire lifespan in all analyzed regions. *ATP1A2* and *ATP1A3* have opposite expression patterns. Expression pattern of *ATP1A2* closely follows the expression pattern of *SLC12A5* (cf. Fig. 1), while *ATP1A3* has the opposite expression pattern (higher prenatal and lower postnatal level of expression).

Fig 6. Spatiotemporal expression patterns of *ATP1B1-4* in the human brain.

The microarray expression data were analyzed for all four ATP1B (encoding Na-K ATPase β subunits 1-4) family members in 16 brain regions and at 13 different developmental periods (see Suppl. Table 1). Three members of the family (*ATP1B1-3*) are expressed in the human brain, while *ATP1B4* is not expressed in the human brain at any period. *ATP1B1* and *ATP1B2* exhibit similar expression pattern as *SLC12A5*, while *ATP1B3* exhibits similar expression pattern as *ATP1A3* (higher prenatal and lower postnatal level of expression).

Fig 7. Spatiotemporal expression patterns of *SYP and DLG4* in the human brain

The microarray expression data were analyzed for *SYP* (encoding synaptophysin) *and DLG4* (encoding PSD-95) in 16 brain regions and at 13 different developmental periods (see Suppl. Table 1). *SYP AND DLG4* are expressed in all examined regions from 10 PCW. Note that expression pattern of *SYP* follows up-regulation of KCC2 expression in the neocortex. *DLG4* is expressed at high levels throughout the development, however it undergoes upregulation which correlates with the *SLC12A5* upregulation.

Fig 8. Spatiotemporal expression patterns of *CAST, CAPN1, CAPN2 and CAPNS1 in the human brain.*

The microarray expression data were analyzed for *CAST* (encoding calpastatin), *CAPN1* (encoding large subunit of calpain 1), *CAPN2* (encoding large subunit of calpain 2) and *CAPNS1* (encoding small subunit of calpains 1-2) in 16 brain regions and at 13 different developmental periods (see Suppl. Table 1). *CAPN1* and *CAPN2* are expressed continuously throughout entire lifespan with *CAPN1* exhibiting higher prenatal and *CAPN2* higher postnatal levels of expression. Note that *CAST* exhibits very low expression levels especially during the prenatal period and is up-regulated in the postnatal period. *CAPNS1* is expressed at high at high levels throughout entire lifespan.

References

Aguado F, Carmona MA, Pozas E, Aguilo A, Martinez-Guijarro FJ, Alcantara S, Borrell V, Yuste R, Ibanez CF, Soriano E. 2003. BDNF regulates spontaneous correlated activity at early developmental stages by increasing synaptogenesis and expression of the K+/Cl- co-transporter KCC2. Development 130:1267-1280.

Allendoerfer KL, Shatz CJ. 1994. The Subplate, A Transient Neocortical Structure: Its Role in the Development of Connections between Thalamus and Cortex. Annu Rev Neurosci 17:185-218.

Amini M, Ma CL, Farazifard R, Zhu G, Zhang Y, Vanderluit J, Zoltewicz JS, Hage F, Savitt JM, Lagace DC, Slack RS, Beique JC, Baudry M, Greer PA, Bergeron R, Park DS. 2013. Conditional disruption of calpain in the CNS alters dendrite morphology, impairs LTP, and promotes neuronal survival following injury. J Neurosci 33:5773-5784.

Andres AL, Regev L, Phi L, Seese RR, Chen Y, Gall CM, Baram TZ. 2013. NMDA receptor activation and calpain contribute to disruption of dendritic spines by the stress neuropeptide CRH. J Neurosci 33:16945-16960.

Aronica E, Boer K, Redeker S, Spliet WG, van Rijen PC, Troost D, Gorter JA. 2007. Differential expression patterns of chloride transporters, Na+-K+-2Cl--cotransporter and K+-Cl--cotransporter, in epilepsy-associated malformations of cortical development. Neuroscience 145:185-196.

Balakrishnan V, Becker M, Löhrke S, Nothwang HG, Güresir E, Friauf E. 2003. Expression and function of chloride transporters during development of inhibitory neurotransmission in the auditory brainstem. J Neurosci 23:4134-4145.

Baldi R, Varga C, Tamas G. 2010. Differential distribution of KCC2 along the axo-somato-dendritic axis of hippocampal principal cells. Eur J Neurosci 32:1319-1325.

Baudry M, Chou MM, Bi X. 2013. Targeting calpain in synaptic plasticity. Expert Opin Ther Targets 17:579-592.

Bayatti N, Moss JA, Sun L, Ambrose P, Ward JF, Lindsay S, Clowry GJ. 2008. A molecular neuroanatomical study of the developing human neocortex from 8 to 17 postconceptional weeks revealing the early differentiation of the subplate and subventricular zone. Cereb Cortex 18:1536-1548.

Ben-Ari Y, Gaiarsa JL, Tyzio R, Khazipov R. 2007. GABA: a pioneer transmitter that excites immature neurons and generates primitive oscillations. Physiol Rev 87:1215-1284.

Blaesse P, Airaksinen MS, Rivera C, Kaila K. 2009. Cation-chloride cotransporters and neuronal function. Neuron 61:820-838.

Blaesse P, Guillemin I, Schindler J, Schweizer M, Delpire E, Khiroug L, Friauf E, Nothwang HG. 2006. Oligomerization of KCC2 correlates with development of inhibitory neurotransmission. J Neurosci 26:10407-10419.

Blaesse P, Schmidt T. 2014. K-Cl cotransporter KCC2-a moonlighting protein in excitatory and inhibitory synapse development and function. Pflugers Arch DOI: 10.1007/s00424-014-1547-6.

Blomgren K, Hallin U, Andersson AL, Puka-Sundvall M, Bahr BA, McRae A, Saido TC, Kawashima S, Hagberg H. 1999. Calpastatin is up-regulated in response to hypoxia and is a suicide substrate to calpain after neonatal cerebral hypoxia-ischemia. J Biol Chem 274:14046-14052.

Blomgren K, Karlsson JO. 1989. Developmental changes of calpain and calpastatin in rabbit brain. Neurochem Res 14:1149-1152.

Blomgren K, Nilsson E, Karlsson JO. 1989. Calpain and calpastatin levels in different organs of the rabbit. Comp Biochem Physiol B 93:403-407.

Bos R, Sadlaoud K, Boulenguez P, Buttigieg D, Liabeuf S, Brocard C, Haase G, Bras H, Vinay L. 2013. Activation of 5-HT2A receptors upregulates the function of the neuronal K-Cl cotransporter KCC2. Proc Natl Acad Sci U S A 110:348-353.

Calhoun ME, Jucker M, Martin LJ, Thinakaran G, Price DL, Mouton PR. 1996. Comparative evaluation of synaptophysin-based methods for quantification of synapses. J Neurocytol 25:821-828.

Carmona MA, Pozas E, Martinez A, Espinosa-Parrilla JF, Soriano E, Aguado F. 2006. Age-dependent spontaneous hyperexcitability and impairment of GABAergic function in the hippocampus of mice lacking trkB. Cereb Cortex 16:47-63.

Chamma I, Chevy Q, Poncer JC, Levi S. 2012. Role of the neuronal K-Cl co-transporter KCC2 in inhibitory and excitatory neurotransmission. Front Cell Neurosci 6:5.

Chamma I, Heubl M, Chevy Q, Renner M, Moutkine I, Eugene E, Poncer JC, Levi S. 2013. Activity-Dependent Regulation of the K/Cl Transporter KCC2 Membrane Diffusion, Clustering, and Function in Hippocampal Neurons. J Neurosci 33:15488-15503.

Clancy B, Darlington RB, Finlay BL. 2001. Translating developmental time across mammalian species. Neuroscience 105:7-17.

Clayton GH, Owens GC, Wolff JS, Smith RL. 1998. Ontogeny of cation-Cl- cotransporter expression in rat neocortex. Dev Brain Res 109:281-292.

Das A, Wallace GC, Holmes C, McDowell ML, Smith JA, Marshall JD, Bonilha L, Edwards JC, Glazier SS, Ray SK, Banik NL. 2012. Hippocampal tissue of patients with refractory temporal lobe epilepsy is associated with astrocyte activation, inflammation, and altered expression of channels and receptors. Neuroscience 220:237-246.

De Felipe J, Marco P, Fairen A, Jones EG. 1997. Inhibitory synaptogenesis in mouse somatosensory cortex. Cereb Cortex 7:619-634.

Diamond J. 2002. Quantitative evolutionary design. J Physiol 542:337-345.

Dzhala VI, Talos DM, Sdrulla DA, Brumback AC, Mathews GC, Benke TA, Delpire E, Jensen FE, Staley KJ. 2005. NKCC1 transporter facilitates seizures in the developing brain. Nat Med 11:1205-1213.

Eastwood SL, Weickert CS, Webster MJ, Herman MM, Kleinman JE, Harrison PJ. 2006. Synaptophysin protein and mRNA expression in the human hippocampal formation from birth to old age. Hippocampus 16:645-654.

Erecinska M, Cherian S, Silver IA. 2004. Energy metabolism in mammalian brain during development. Prog Neurobiol 73:397-445.

Feng ZH, Hao J, Ye L, Dayao C, Yan N, Yan Y, Chu L, Shi FD. 2011. Overexpression of mu-calpain in the anterior temporal neocortex of patients with intractable epilepsy correlates with clinicopathological characteristics. Seizure 20:395-401.

Fiumelli H, Briner A, Puskarjov M, Blaesse P, Belem BJ, Dayer AG, Kaila K, Martin JL, Vutskits L. 2013. An ion transport-independent role for the cation-chloride cotransporter KCC2 in dendritic spinogenesis in vivo. Cereb Cortex 23:378-388.

Fujii T, Fujita K, Shimizu T, Takeguchi N, Sakai H. 2010. The NH(2)-terminus of K(+)-Cl(-) cotransporter 3a is essential for up-regulation of Na(+),K(+)-ATPase activity. Biochem Biophys Res Commun 399:683-687.

Fujii T, Takahashi Y, Ikari A, Morii M, Tabuchi Y, Tsukada K, Takeguchi N, Sakai H. 2009. Functional association between K+-Cl- cotransporter-4 and H+,K+-ATPase in the apical canalicular membrane of gastric parietal cells. J Biol Chem 284:619-629.

Fujii T, Takahashi Y, Itomi Y, Fujita K, Morii M, Tabuchi Y, Asano S, Tsukada K, Takeguchi N, Sakai H. 2008. K+-Cl- Cotransporter-3a Up-regulates Na+,K+-ATPase in Lipid Rafts of Gastric Luminal Parietal Cells. J Biol Chem 283:6869-6877.

Fujikawa DG. 2005. Prolonged seizures and cellular injury: understanding the connection. Epilepsy Behav 7 Suppl 3:S3-11.

Fujita K, Fujii T, Shimizu T, Takeguchi N, Sakai H. 2012. Role of cholesterol in functional association between K(+)-Cl(-) cotransporter-3a and Na+,K(+)-ATPase. Biochem Biophys Res Commun 424:136-140.

Gagnon KB, Di Fulvio M. 2013. A molecular analysis of the Na(+)-independent cation chloride cotransporters. Cell Physiol Biochem 32:14-31.

Gagnon M, Bergeron MJ, Lavertu G, Castonguay A, Tripathy S, Bonin RP, Perez-Sanchez J, Boudreau D, Wang B, Dumas L, Valade I, Bachand K, Jacob-Wagner M, Tardif C, Kianicka I, Isenring P, Attardo G, Coull JA, De KY. 2013. Chloride extrusion enhancers as novel therapeutics for neurological diseases. Nat Med 19:1524-1528.

Gauvain G, Chamma I, Chevy Q, Cabezas C, Irinopoulou T, Bodrug N, Carnaud M, Levi S, Poncer JC. 2011. The neuronal K-Cl cotransporter KCC2 influences postsynaptic AMPA receptor content and lateral diffusion in dendritic spines. Proc Natl Acad Sci U S A 108:15474-15479.

Goll DE, Thompson VF, Li H, Wei W, Cong J. 2003. The calpain system. Physiol Rev 83:731-801.

Gulyas AI, Sik A, Payne JA, Kaila K, Freund TF. 2001. The KCl cotransporter, KCC2, is highly expressed in the vicinity of excitatory synapses in the rat hippocampus. Eur J Neurosci 13:2205-2217.

Hoerder-Suabedissen A, Molnar Z. 2015. Development, evolution and pathology of neocortical subplate neurons. Nat Rev Neurosci 16:133-146.

Horn Z, Ringstedt T, Blaesse P, Kaila K, Herlenius E. 2010. Premature expression of KCC2 in embryonic mice perturbs neural development by an ion transport-independent mechanism. Eur J Neurosci 31:2142-2155.

Hsu SM, Raine L, Fanger H. 1981. The use of antiavidin antibody and avidin-biotin-peroxidase complex in immunoperoxidase technics. Am J Clin Pathol 75:816-821.

Hübner CA, Lorke DE, Hermans-Borgmeyer I. 2001a. Expression of the Na-K-2Cl-cotransporter NKCC1 during mouse development. Mech Dev 102:267-269.

Hübner CA, Stein V, Hermans-Borgmeyer I, Meyer T, Ballanyi K, Jentsch TJ. 2001b. Disruption of KCC2 reveals an essential role of K-Cl cotransport already in early synaptic inhibition. Neuron 30:515-524.

Huttenlocher PR, Dabholkar AS. 1997. Regional differences in synaptogenesis in human cerebral cortex. J Comp Neurol 387:167-178.

Huttenlocher PR, de Court, Garey LJ, van der Loos H. 1982. Synaptic development in human cerebral cortex. Int J Neurol 16-17:144-154.

Hyde TM, Lipska BK, Ali T, Mathew SV, Law AJ, Metitiri OE, Straub RE, Ye T, Colantuoni C, Herman MM, Bigelow LB, Weinberger DR, Kleinman JE. 2011. Expression of GABA signaling molecules KCC2, NKCC1, and GAD1 in cortical development and schizophrenia. J Neurosci 31:11088-11095.

Ikeda K, Onimaru H, Yamada J, Inoue K, Ueno S, Onaka T, Toyoda H, Arata A, Ishikawa T, Taketo MM, Fukuda A, Kawakami K. 2004. Malfunction of respiratory-related neuronal activity in Na+, K+-ATPase alpha 2 subunit-deficient mice is attributable to abnormal Cl- homeostasis in brainstem neurons. J Neurosci 24:10693-10701.

Inoue K, Yamada J, Ueno S, Fukuda A. 2006. Brain-type creatine kinase activates neuron-specific K+-Cl- co-transporter KCC2. J Neurochem 96:598-608.

Jansen LA, Peugh LD, Roden WH, Ojemann JG. 2010. Impaired maturation of cortical GABA(A) receptor expression in pediatric epilepsy. Epilepsia 51:1456-1467.

Jantzie LL, Getsy PM, Firl DJ, Wilson CG, Miller RH, Robinson S. 2014. Erythropoietin attenuates loss of potassium chloride co-transporters following prenatal brain injury. Mol Cell Neurosci 61:152-162.

Judas M, Simic G, Petanjek Z, Jovanov-Milosevic N, Pletikos M, Vasung L, Vuksic M, Kostovic I. 2011. The Zagreb Collection of human brains: a unique, versatile, but underexploited resource for the neuroscience community. Ann N Y Acad Sci 1225 Suppl 1:E105-E130.

Juraska JM. 1982. The development of pyramidal neurons after eye opening in the visual cortex of hooded rats: a quantitative study. J Comp Neurol 212:208-213.

Kahle KT, Deeb TZ, Puskarjov M, Silayeva L, Liang B, Kaila K, Moss SJ. 2013. Modulation of neuronal activity by phosphorylation of the K-Cl cotransporter KCC2. Trends Neurosci 36:726-737.

Kahle KT, Merner ND, Friedel P, Silayeva L, Liang B, Khanna A, Shang Y, Lachance-Touchette P, Bourassa C, Levert A, Dion PA, Walcott B, Spiegelman D, Dionne-Laporte A, Hodgkinson A, Awadalla P, Nikbakht H, Majewski J, Cossette P, Deeb TZ, Moss SJ, Medina I, Rouleau GA. 2014. Genetically encoded impairment of neuronal KCC2 cotransporter function in human idiopathic generalized epilepsy. EMBO Rep 15:766-774.

Kaila K, Price TJ, Payne JA, Puskarjov M, Voipio J. 2014a. Cation-chloride cotransporters in neuronal development, plasticity and disease. Nat Rev Neurosci 15:637-654.

Kaila K, Ruusuvuori E, Seja P, Voipio J, Puskarjov M. 2014b. GABA actions and ionic plasticity in epilepsy. Curr Opin Neurobiol 26:34-41.

Kang HJ, Kawasawa YI, Cheng F, Zhu Y, Xu X, Li M, Sousa AM, Pletikos M, Meyer KA, Sedmak G, Guennel T, Shin Y, Johnson MB, Krsnik Z, Mayer S, Fertuzinhos S, Umlauf S, Lisgo SN, Vortmeyer A, Weinberger DR, Mane S, Hyde TM, Huttner A, Reimers M, Kleinman JE, Sestan N. 2011. Spatio-temporal transcriptome of the human brain. Nature 478:483-489.

Kanold PO, Luhmann HJ. 2010. The subplate and early cortical circuits. Annu Rev Neurosci 33:23-48.

Kanold PO, Shatz CJ. 2006. Subplate neurons regulate maturation of cortical inhibition and outcome of ocular dominance plasticity. Neuron 51:627-638.

Kawamura M, Nakajima W, Ishida A, Ohmura A, Miura S, Takada G. 2005. Calpain inhibitor MDL 28170 protects hypoxic-ischemic brain injury in neonatal rats by inhibition of both apoptosis and necrosis. Brain Res 1037:59-69.

Khalilov I, Chazal G, Chudotvorova I, Pellegrino C, Corby S, Ferrand N, Gubkina O, Nardou R, Tyzio R, Yamamoto S, Jentsch TJ, Hubner CA, Gaiarsa JL, Ben-Ari Y, Medina I. 2011. Enhanced Synaptic Activity and Epileptiform Events in the Embryonic KCC2 Deficient Hippocampus. Front Cell Neurosci 5:23.

Khazipov R, Luhmann HJ. 2006. Early patterns of electrical activity in the developing cerebral cortex of humans and rodents. Trends Neurosci 29:414-418.

Khirug S, Ahmad F, Puskarjov M, Afzalov R, Kaila K, Blaesse P. 2010. A single seizure episode leads to rapid functional activation of KCC2 in the neonatal rat hippocampus. J Neurosci 30:12028-12035.

Khirug S, Huttu K, Ludwig A, Smirnov S, Voipio J, Rivera C, Kaila K, Khiroug L. 2005. Distinct properties of functional KCC2 expression in immature mouse hippocampal neurons in culture and in acute slices. Eur J Neurosci 21:899-904.

Khirug S, Yamada J, Afzalov R, Voipio J, Khiroug L, Kaila K. 2008. GABAergic depolarization of the axon initial segment in cortical principal neurons is caused by the Na-K-2Cl cotransporter NKCC1. J Neurosci 28:4635-4639.

Kostovic I, Judas M. 2002. Correlation between the sequential ingrowth of afferents and transient patterns of cortical lamination in preterm infants. Anat Rec 267:1-6.

Kostovic I, Judas M. 2006. Prolonged coexistence of transient and permanent circuitry elements in the developing cerebral cortex of fetuses and preterm infants. Dev Med Child Neurol 48:388-393.

Kostovic I, Judas M. 2007. Transient patterns of cortical lamination during prenatal life: do they have implications for treatment? Neurosci Biobehav Rev 31:1157-1168.

Kostovic I, Judas M, Kostovic-Knezevic L, Simic G, Delalle I, Chudy D, Sajin B, Petanjek Z. 1991. Zagreb research collection of human brains for developmental neurobiologists and clinical neuroscientists. Int J Dev Biol 35:215-230.

Kostovic I, Rakic P. 1990. Developmental history of the transient subplate zone in the visual and somatosensory cortex of the macaque monkey and human brain. J Comp Neurol 297:441-470.

Kovacs K, Basu K, Rouiller I, Sik A. 2014. Regional differences in the expression of K(+)-Cl(-) 2 cotransporter in the developing rat cortex. Brain Struct Funct 219:527-538.

Leinekugel X, Khazipov R, Cannon R, Hirase H, Ben Ari Y, Buzsaki G. 2002. Correlated bursts of activity in the neonatal hippocampus in vivo. Science 296:2049-2052.

Li H, Khirug S, Cai C, Ludwig A, Blaesse P, Kolikova J, Afzalov R, Coleman SK, Lauri S, Airaksinen MS, Keinanen K, Khiroug L, Saarma M, Kaila K, Rivera C. 2007. KCC2 interacts with the dendritic cytoskeleton to promote spine development. Neuron 56:1019-1033.

Li H, Tornberg J, Kaila K, Airaksinen MS, Rivera C. 2002. Patterns of cation-chloride cotransporter expression during embryonic rodent CNS development. Eur J Neurosci 16:2358-2370.

Li Y, Bondada V, Joshi A, Geddes JW. 2009. Calpain 1 and Calpastatin expression is developmentally regulated in rat brain. Exp Neurol 220:316-319.

Liu J, Liu MC, Wang KK. 2008. Calpain in the CNS: from synaptic function to neurotoxicity. Sci Signal 1:re1.

Liu Q, Wong-Riley MT. 2012. Postnatal development of Na(+)-K(+)-2Cl(-) co-transporter 1 and K(+)-Cl(-) co-transporter 2 immunoreactivity in multiple brain stem respiratory nuclei of the rat. Neuroscience 210:1-20.

Löscher W, Klitgaard H, Twyman RE, Schmidt D. 2013a. New avenues for anti-epileptic drug discovery and development. Nat Rev Drug Discov 12:757-776.

Löscher W, Puskarjov M, Kaila K. 2013b. Cation-chloride cotransporters NKCC1 and KCC2 as potential targets for novel antiepileptic and antiepileptogenic treatments. Neuropharmacology 69:62-74.

Lu X, Rong Y, Baudry M. 2000. Calpain-mediated degradation of PSD-95 in developing and adult rat brain. Neurosci Lett 286:149-153.

Luberg K, Wong J, Weickert CS, Timmusk T. 2010. Human TrkB gene: novel alternative transcripts, protein isoforms and expression pattern in the prefrontal cerebral cortex during postnatal development. J Neurochem 113:952-964.

Ludwig A, Li H, Saarma M, Kaila K, Rivera C. 2003. Developmental up-regulation of KCC2 in the absence of GABAergic and glutamatergic transmission. Eur J Neurosci 18:3199-3206.

Ludwig A, Uvarov P, Pellegrino C, Thomas-Crusells J, Schuchmann S, Saarma M, Airaksinen MS, Rivera C. 2011a. Neurturin evokes MAPK-dependent upregulation of Egr4 and KCC2 in developing neurons. Neural Plast 2011:1-8.

Ludwig A, Uvarov P, Soni S, Thomas-Crusells J, Airaksinen MS, Rivera C. 2011b. Early growth response 4 mediates BDNF induction of potassium chloride cotransporter 2 transcription. J Neurosci 31:644-649.

Lynch G, Baudry M. 1984. The biochemistry of memory: a new and specific hypothesis. Science 224:1057-1063.

Markkanen M, Uvarov P, Airaksinen MS. 2008. Role of upstream stimulating factors in the transcriptional regulation of the neuron-specific K-Cl cotransporter KCC2. Brain Res 1236:8-15.

Marty S, Wehrle R, Alvarez-Leefmans FJ, Gasnier B, Sotelo C. 2002. Postnatal maturation of Na+, K+, 2Cl- cotransporter expression and inhibitory synaptogenesis in the rat hippocampus: an immunocytochemical analysis. Eur J Neurosci 15:233-245.

Mikawa S, Wang C, Shu F, Wang T, Fukuda A, Sato K. 2002. Developmental changes in KCC1, KCC2 and NKCC1 mRNAs in the rat cerebellum. Dev Brain Res 136:93-100.

Molliver ME, Kostovic I, van der Loos H. 1973. The development of synapses in cerebral cortex of the human fetus. Brain Res 50:403-407.

Morita Y, Callicott JH, Testa LR, Mighdoll MI, Dickinson D, Chen Q, Tao R, Lipska BK, Kolachana B, Law AJ, Ye T, Straub RE, Weinberger DR, Kleinman JE, Hyde TM. 2014. Characteristics of the Cation Cotransporter NKCC1 in Human Brain: Alternate Transcripts, Expression in Development, and Potential Relationships to Brain Function and Schizophrenia. J Neurosci 34:4929-4940.

Mrzljak L, Uylings HB, Kostovic I, Van Eden CG. 1988. Prenatal development of neurons in the human prefrontal cortex: I. A qualitative Golgi study. J Comp Neurol 271:355-386.

Mrzljak L, Uylings HB, Kostovic I, Van Eden CG. 1992. Prenatal development of neurons in the human prefrontal cortex. II. A quantitative Golgi study. J Comp Neurol 316:485-496.

Mrzljak L, Uylings HB, Van Eden CG, Judas M. 1990. Neuronal development in human prefrontal cortex in prenatal and postnatal stages. Prog Brain Res 85:185-222.

Ostwald K, Hagberg H, Andine P, Karlsson JO. 1993. Upregulation of calpain activity in neonatal rat brain after hypoxic-ischemia. Brain Res 630:289-294.

Park H, Poo MM. 2013. Neurotrophin regulation of neural circuit development and function. Nat Rev Neurosci 14:7-23.

Payne JA, Rivera C, Voipio J, Kaila K. 2003. Cation-chloride co-transporters in neuronal communication, development and trauma. Trends Neurosci 26:199-206.

Petanjek Z, Judas M, Simic G, Rasin MR, Uylings HB, Rakic P, Kostovic I. 2011. Extraordinary neoteny of synaptic spines in the human prefrontal cortex. Proc Natl Acad Sci U S A 108:13281-13286.

Plotkin MD, Snyder EY, Hebert SC, Delpire E. 1997. Expression of the Na-K-2Cl cotransporter is developmentally regulated in postnatal rat brains: a possible mechanism underlying GABA's excitatory role in immature brain. J Neurobiol 33:781-795.

Pressler RM, Boylan GB, Marlow N, Blennow M, Chiron C, Cross JH, De Vries LS, Hallberg B, Hellstrom-Westas L, Jullien V, Livingstone V, Mangum B, Murphy B, Murray D, Pons G, Rennie J, Swarte R, Toet MC, Vanhatalo S, Zohar S. 2015. Bumetanide for the treatment of seizures in newborn babies with hypoxic ischaemic encephalopathy (NEMO): an open-label, dose finding, and feasibility phase 1/2 trial. Lancet Neurol 14:469-477.

Puskarjov M, Ahmad F, Kaila K, Blaesse P. 2012. Activity-dependent cleavage of the K-Cl cotransporter KCC2 mediated by calcium-activated protease calpain. J Neurosci 32:11356-11364.

Puskarjov M, Ahmad F, Khirug S, Sivakumaran S, Kaila K, Blaesse P. 2015. BDNF is required for seizure-induced but not developmental up-regulation of KCC2 in the neonatal hippocampus. Neuropharmacology 88:103-109.

Puskarjov M, Kahle KT, Ruusuvuori E, Kaila K. 2014a. Pharmacotherapeutic targeting of cation-chloride cotransporters in neonatal seizures. Epilepsia 55:806-818.

Puskarjov M, Seja P, Heron SE, Williams TC, Ahmad F, Iona X, Oliver KL, Grinton BE, Vutskits L, Scheffer IE, Petrou S, Blaesse P, Dibbens LM, Berkovic SF, Kaila K. 2014b. A variant of KCC2 from patients with febrile seizures impairs neuronal Cl^- extrusion and dendritic spine formation. EMBO Rep 15:723-729.

Randall J, Thorne T, Delpire E. 1997. Partial cloning and characterization of Slc12a2: the gene encoding the secretory Na+-K+-2Cl- cotransporter. Am J Physiol 273:C1267-C1277.

Rivera C, Voipio J, Payne JA, Ruusuvuori E, Lahtinen H, Lamsa K, Pirvola U, Saarma M, Kaila K. 1999. The K+/Cl- co-transporter KCC2 renders GABA hyperpolarizing during neuronal maturation. Nature 397:251-255.

Robinson S, Mikolaenko I, Thompson I, Cohen ML, Goyal M. 2010. Loss of cation-chloride cotransporter expression in preterm infants with white matter lesions: implications for the pathogenesis of epilepsy. J Neuropathol Exp Neurol 69:565-572.

Romanczyk TB, Weickert CS, Webster MJ, Herman MM, Akil M, Kleinman JE. 2002. Alterations in trkB mRNA in the human prefrontal cortex throughout the lifespan. Eur J Neurosci 15:269-280.

Rosenkranz K, May C, Meier C, Marcus K. 2012. Proteomic analysis of alterations induced by perinatal hypoxic-ischemic brain injury. J Proteome Res 11:5794-5803.

Salin-Cantegrel A, Shekarabi M, Holbert S, Dion P, Rochefort D, Laganiere J, Dacal S, Hince P, Karemera L, Gaspar C, Lapointe JY, Rouleau GA. 2008. HMSN/ACC truncation mutations disrupt brain-type creatine kinase-dependant activation of K+/Cl- cotransporter 3. Hum Mol Genet 17:2703-2711.

Shamraj OI, Lingrel JB. 1994. A putative fourth Na+,K(+)-ATPase alpha-subunit gene is expressed in testis. Proc Natl Acad Sci U S A 91:12952-12956.

Shimizu-Okabe C, Yokokura M, Okabe A, Ikeda M, Sato K, Kilb W, Luhmann HJ, Fukuda A. 2002. Layer-specific expression of Cl- transporters and differential [Cl-]i in newborn rat cortex. NeuroReport 13:2433-2437.

Sierra-Paredes G, Cornes JM, Sierra-Marcuno G. 1999. Calpain inhibitor I retards seizure offset in the hippocampus of freely moving rats. Neurosci Lett 263:165-168.

Simonson L, Baudry M, Siman R, Lynch G. 1985. Regional distribution of soluble calcium activated proteinase activity in neonatal and adult rat brain. Brain Res 327:153-159.

Stein V, Hermans-Borgmeyer I, Jentsch TJ, Hübner CA. 2004. Expression of the KCl cotransporter KCC2 parallels neuronal maturation and the emergence of low intracellular chloride. J Comp Neurol 468:57-64.

Sun C, Zhang L, Chen G. 2013. An unexpected role of neuroligin-2 in regulating KCC2 and GABA functional switch. Mol Brain 6:23.

Sun D, Murali SG. 1999. Na+-K+-2Cl- cotransporter in immature cortical neurons: A role in intracellular Cl- regulation. J Neurophysiol 81:1939-1948.

Szabadics J, Varga C, Molnar G, Olah S, Barzo P, Tamas G. 2006. Excitatory effect of GABAergic axo-axonic cells in cortical microcircuits. Science 311:233-235.

Takayama C, Inoue Y. 2006. Developmental localization of potassium chloride co-transporter 2 in granule cells of the early postnatal mouse cerebellum with special reference to the synapse formation. Neuroscience 143:757-767.

Takayama C, Inoue Y. 2010. Developmental localization of potassium chloride co-transporter 2 (KCC2), GABA and vesicular GABA transporter (VGAT) in the postnatal mouse somatosensory cortex. Neurosci Res 67:137-148.

Tokhtaeva E, Clifford RJ, Kaplan JH, Sachs G, Vagin O. 2012. Subunit isoform selectivity in assembly of Na,K-ATPase α-β heterodimers. J Biol Chem 287:26115-26125.

Töllner K, Brandt C, Töpfer M, Brunhofer G, Erker T, Gabriel M, Feit PW, Lindfors J, Kaila K, Löscher W. 2014. A novel prodrug-based strategy to increase effects of bumetanide in epilepsy. Ann Neurol 75:550-562.

Uvarov P, Llano O, Ludwig A, Airaksinen MS, Rivera C. 2013. Multiple roles of KCC2 in the developing brain. In: Rubenstein JLR, Rakic P, editors. Cellular migration and formation of neuronal connections. San Diego: Academic Press. p 975-998.

Uvarov P, Ludwig A, Markkanen M, Rivera C, Airaksinen MS. 2006. Upregulation of the neuron-specific K+/Cl- cotransporter expression by transcription factor early growth response 4. J Neurosci 26:13463-13473.

Uvarov P, Ludwig A, Markkanen M, Soni S, Hubner CA, Rivera C, Airaksinen MS. 2009. Coexpression and heteromerization of two neuronal K-Cl cotransporter isoforms in neonatal brain. J Biol Chem 284:13696-13704.

Uvarov P, Pruunsild P, Timmusk T, Airaksinen MS. 2005. Neuronal K+/Cl- co-transporter (KCC2) transgenes lacking neurone restrictive silencer element recapitulate CNS neurone-specific expression and developmental up-regulation of endogenous KCC2 gene. J Neurochem 95:1144-1155.

Vanhatalo S, Kaila K. 2006. Development of neonatal EEG activity: from phenomenology to physiology. Semin Fetal Neonatal Med 11:471-478.

Vanhatalo S, Palva JM, Andersson S, Rivera C, Voipio J, Kaila K. 2005. Slow endogenous activity transients and developmental expression of K+-Cl- cotransporter 2 in the immature human cortex. Eur J Neurosci 22:2799-2804.

Vibat CRT, Holland MJ, Kang JJ, Putney LK, O'Donnell ME. 2001. Quantitation of Na+-K+-2Cl(-) cotransport splice variants in human tissues using kinetic polymerase chain reaction. Anal Biochem 298:218-230.

Volpe J. 2008. Neurology of the newborn. Philadelphia: Saunders.

Wang C, Shimizu-Okabe C, Watanabe K, Okabe A, Matsuzaki H, Ogawa T, Mori N, Fukuda A, Sato K. 2002. Developmental changes in KCC1, KCC2, and NKCC1 mRNA expressions in the rat brain. Brain Res Dev Brain Res 139:59-66.

Webster MJ, Herman MM, Kleinman JE, Shannon WC. 2006. BDNF and trkB mRNA expression in the hippocampus and temporal cortex during the human lifespan. Gene Expr Patterns 6:941-951.

Yamada J, Okabe A, Toyoda H, Kilb W, Luhmann HJ, Fukuda A. 2004. Cl- uptake promoting depolarizing GABA actions in immature rat neocortical neurones is mediated by NKCC1. J Physiol 557:829-841.

Yan Y, Dempsey RJ, Sun D. 2001. Expression of Na+-K+-Cl- cotransporter in rat brain during development and its localization in mature astrocytes. Brain Res 911:43-55.

Yang J, Weimer RM, Kallop D, Olsen O, Wu Z, Renier N, Uryu K, Tessier-Lavigne M. 2013. Regulation of axon degeneration after injury and in development by the endogenous calpain inhibitor calpastatin. Neuron 80:1175-1189.

Yeo M, Berglund K, Augustine G, Liedtke W. 2009. Novel repression of Kcc2 transcription by REST-RE-1 controls developmental switch in neuronal chloride. J Neurosci 29:14652-14662.

Zhang LL, Fina ME, Vardi N. 2006. Regulation of KCC2 and NKCC during development: Membrane insertion and differences between cell types. J Comp Neurol 499:132-143.

Zhou HY, Chen SR, Byun HS, Chen H, Li L, Han HD, Lopez-Berestein G, Sood AK, Pan HL. 2012. N-methyl-D-aspartate receptor- and calpain-mediated proteolytic cleavage of K+-Cl- cotransporter-2 impairs spinal chloride homeostasis in neuropathic pain. J Biol Chem 287:33853-33864.

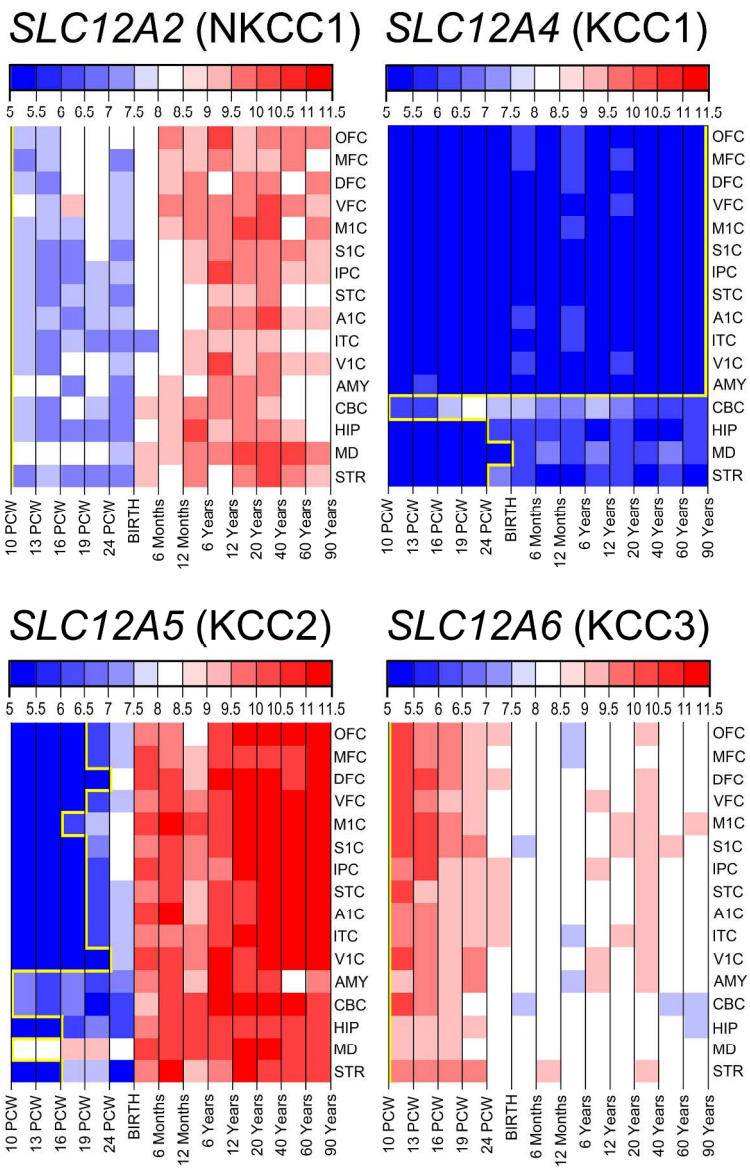

Fig. 1. Spatiotemporal expression patterns of SLC12A family in the human brain.
The microarray expression data were analyzed for all 9 members of the SLC12 family in 16 brain regions and at 13 different developmental periods (see Suppl. Table 1). Five CCCs (SLC12A1 [encoding NKCC2], SLC12A3 [NCC], SLC12A7 [KCC4], SLC12A9 [CIP1], SLC12A8 [CCC9]) were not expressed in the human brain in any region or at any period (Suppl. Fig. 1). Remaining four CCCs (SLC12A2 [NKCC1], SLC12A4-6 [KCC1-3]) exhibited diverse spatiotemporal patterns of expression. NKCC1 and KCC3 were expressed in all regions at all periods, while KCC1 and KCC2 had specific patterns of expression (for details see text). Yellow line represents border between expressed (right) and unexpressed (left) samples. Note that in the majority of neocortical regions the onset of KCC2 expression occurs between 19 and 24 PCW.

183x289mm (300 x 300 DPI)

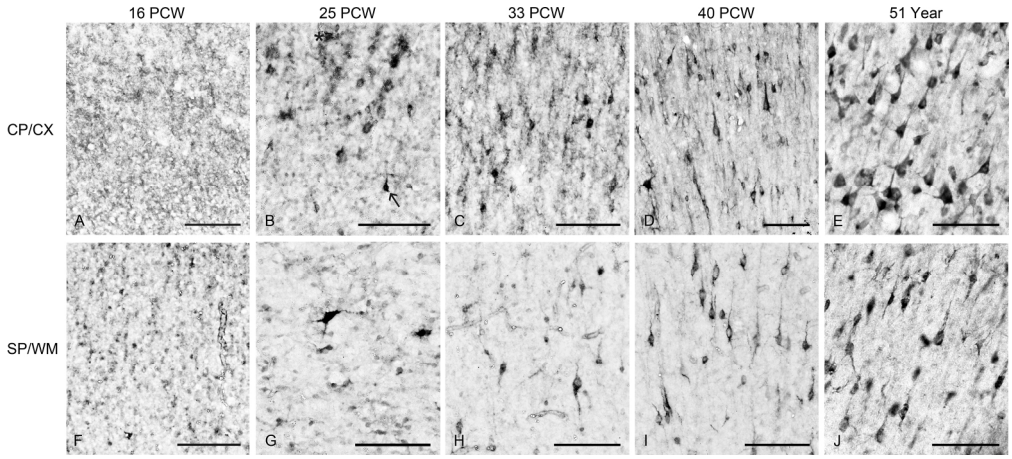

Fig. 2. Developmental expression pattern of KCC2 immunoreactivity in the neocortex. At 16 PCW no KCC2-immunoreactive (KCC2-ir) neurons were observed either in cortical plate (A) or subplate (F). KCC2-ir was present in the neocortex from 25 PCW onwards in both the cortical plate (B) and the subplate (G). KCC2-ir neurons at 33 PCW (C, H), 40 PCW (D, I) and 51 years (E, J). KCC2-ir was also present in the adult subcortical white matter interstitial neurons (H). Note the difference between KCC2-ir neuron (arrow in B) and staining artefact (asterisk in B). Bar = 100 μm.

199x89mm (300 x 300 DPI)

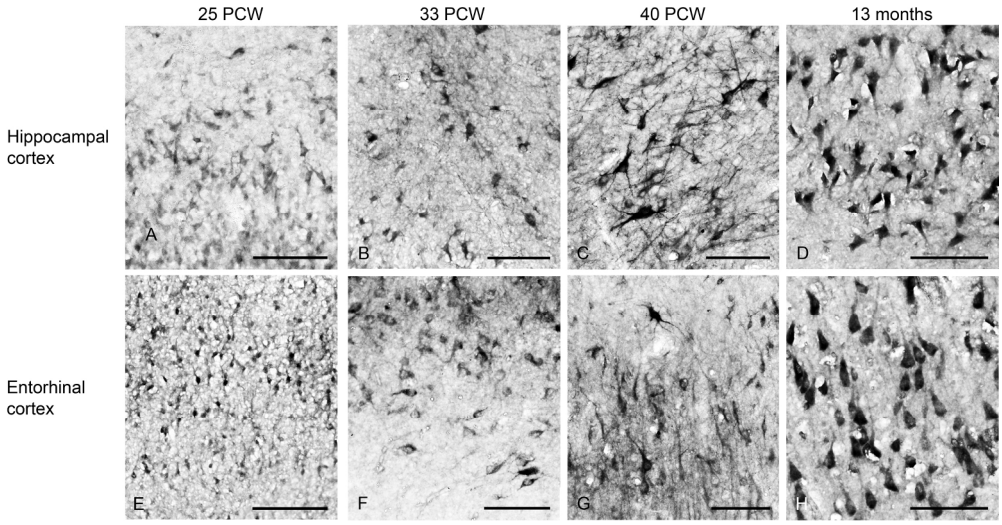

Fig. 3. Developmental expression pattern of KCC2 immunoreactivity in the hippocampus and the entorhinal cortex.
KCC2-ir neurons were observed in the hippocampus (stratum pyramidale) and the entorhinal cortex (layer 3-5) at 25 PCW (A, E), 33 PCW (B, F), 40 PCW (C, G) and 13 months (D, H). Bar = 100 μm.

209x107mm (300 x 300 DPI)

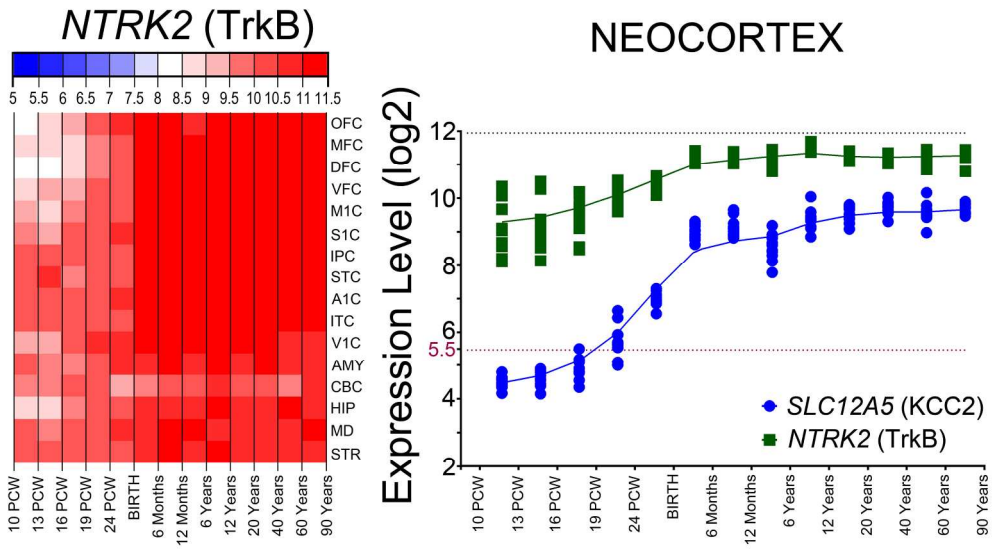

Fig. 4. Spatiotemporal expression patterns of NTRK2 in the human brain.
The microarray expression data were analyzed for NTRK2 (encoding TrkB) in 16 brain regions and at 13 different developmental periods (see Suppl. Table 1). NTRK2 is expressed in all examined regions from 10 PCW. Note that expression pattern of NTRK2 follows up-regulation of KCC2 expression in the neocortex.

209x123mm (300 x 300 DPI)

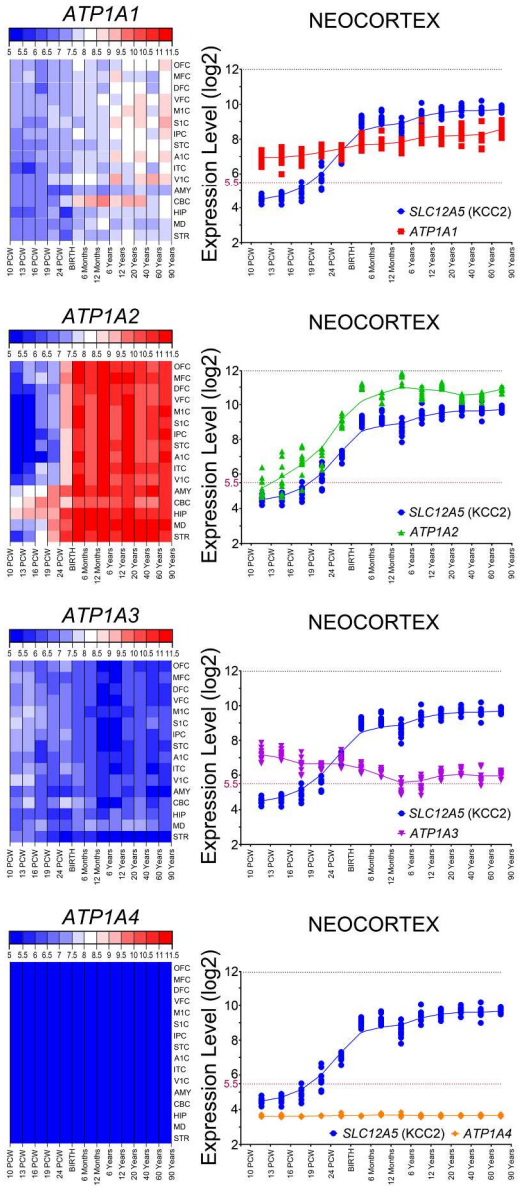

Fig 5. Spatiotemporal expression patterns of ATP1A1-4 in the human brain.
The microarray expression data were analyzed for all 4 ATP1A (encoding Na-K ATPase α subunits 1 4) family members in 16 brain regions and at 13 different developmental periods (see Suppl. Table 1). Three members of the family (ATP1A1-3) are expressed in the human brain, while ATP1A4 is not expressed in the human brain at any period. ATP1A1 starts to be expressed from 10 PCW throughout entire lifespan in all analyzed regions. ATP1A2 and ATP1A3 have opposite expression patterns. Expression pattern of ATP1A2 closely follows the expression pattern of SLC12A5 (cf. Fig. 1), while ATP1A3 has the opposite expression pattern (higher prenatal and lower postnatal level of expression).

124x289mm (300 x 300 DPI)

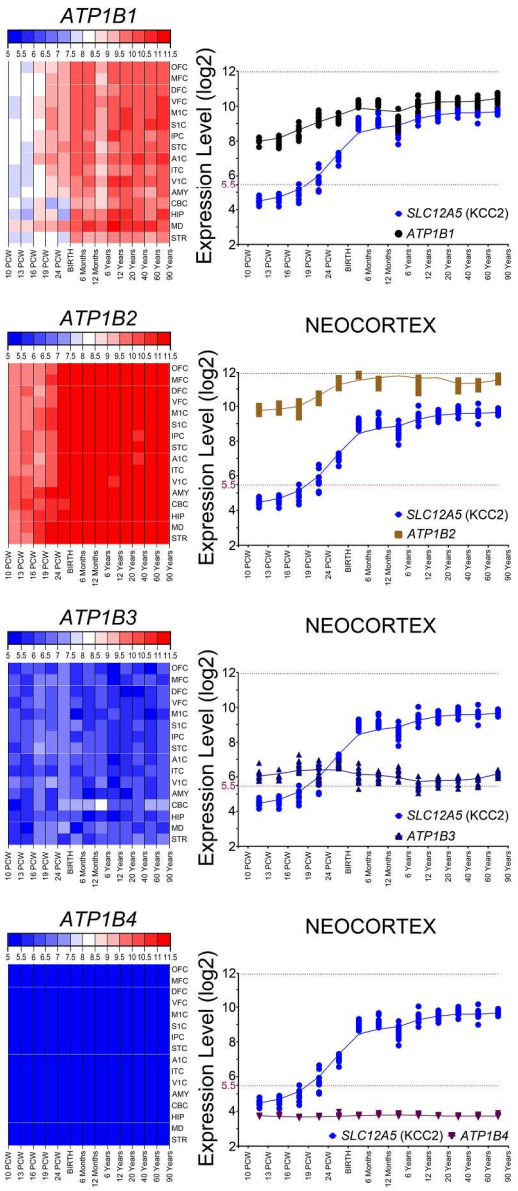

Fig 6. Spatiotemporal expression patterns of ATP1B1-4 in the human brain.
The microarray expression data were analyzed for all four ATP1B (encoding Na-K ATPase β subunits 1-4) family members in 16 brain regions and at 13 different developmental periods (see Suppl. Table 1). Three members of the family (ATP1B1 3) are expressed in the human brain, while ATP1B4 is not expressed in the human brain at any period. ATP1B1 and ATP1B2 exhibit similar expression pattern as SLC12A5, while ATP1B3 exhibits similar expression pattern as ATP1A3 (higher prenatal and lower postnatal level of expression).

125x289mm (300 x 300 DPI)

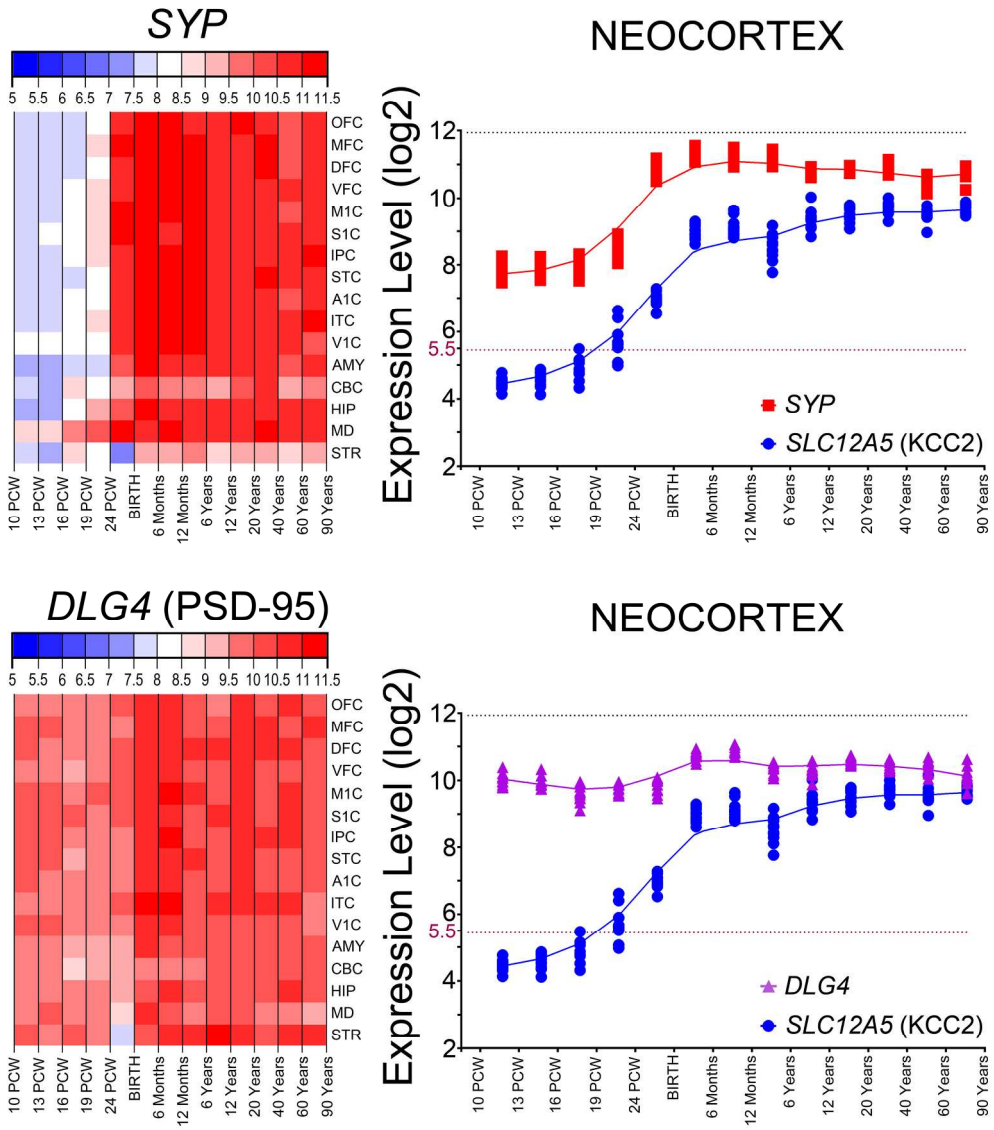

Fig 7. Spatiotemporal expression patterns of SYP and DLG4 in the human brain
The microarray expression data were analyzed for SYP (encoding synaptophysin) and DLG4 (encoding PSD-95) in 16 brain regions and at 13 different developmental periods (see Suppl. Table 1). SYP AND DLG4 are expressed in all examined regions from 10 PCW. Note that expression pattern of SYP follows up-regulation of KCC2 expression in the neocortex. DLG4 is expressed at high levels throughout the development, however it undergoes upregulation which correlates with the SLC12A5 upregulation.

209x239mm (300 x 300 DPI)

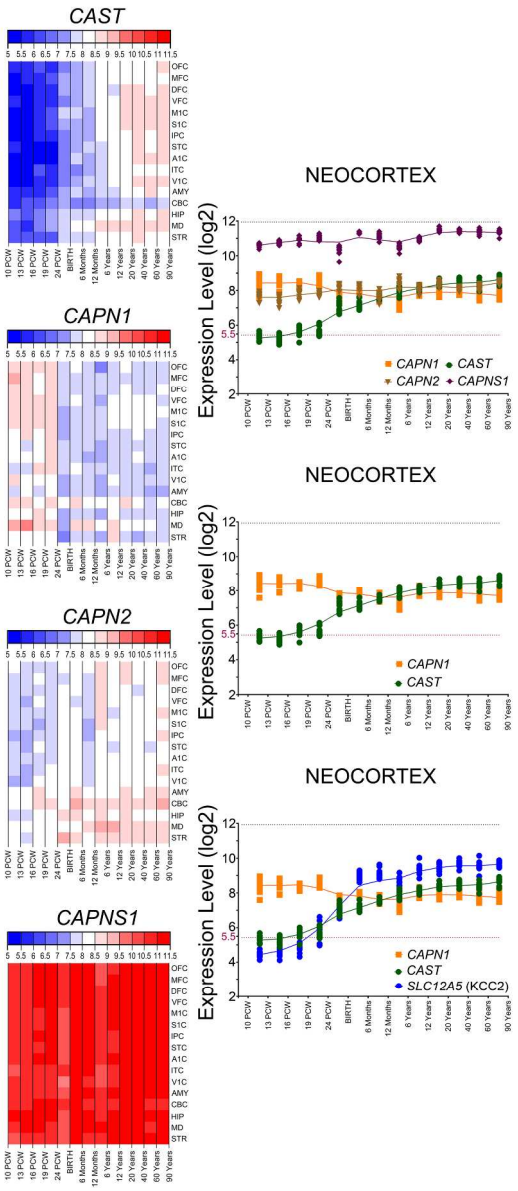

Fig 8. Spatiotemporal expression patterns of CAST, CAPN1, CAPN2 and CAPNS1 in the human brain. The microarray expression data were analyzed for CAST (encoding calpastatin), CAPN1 (encoding large subunit of calpain 1), CAPN2 (encoding large subunit of calpain 2) and CAPNS1 (encoding small subunit of calpains 1-2) in 16 brain regions and at 13 different developmental periods (see Suppl. Table 1). CAPN1 and CAPN2 are expressed continuously throughout entire lifespan with CAPN1 exhibiting higher prenatal and CAPN2 higher postnatal levels of expression. Note that CAST exhibits very low expression levels especially during the prenatal period and is up-regulated in the postnatal period. CAPNS1 is expressed at high at high levels throughout entire lifespan.

125x289mm (300 x 300 DPI)

Supplementary Figure 1. **Spatiotemporal expression patterns of *SLC12A family* in the human brain.**

The microarray expression data were analyzed for all 9 members of the SLC12 family in 16 brain regions and at 13 different developmental periods (see Suppl. Table 1). Five CCCs (*SLC12A1* [encoding NKCC2], *SLC12A3* [NCC], *SLC12A7* [KCC4], *SLC12A9* [CIP1], *SLC12A8* [CCC9]) were not expressed in the human brain in any region or at any period. For details see the main text.

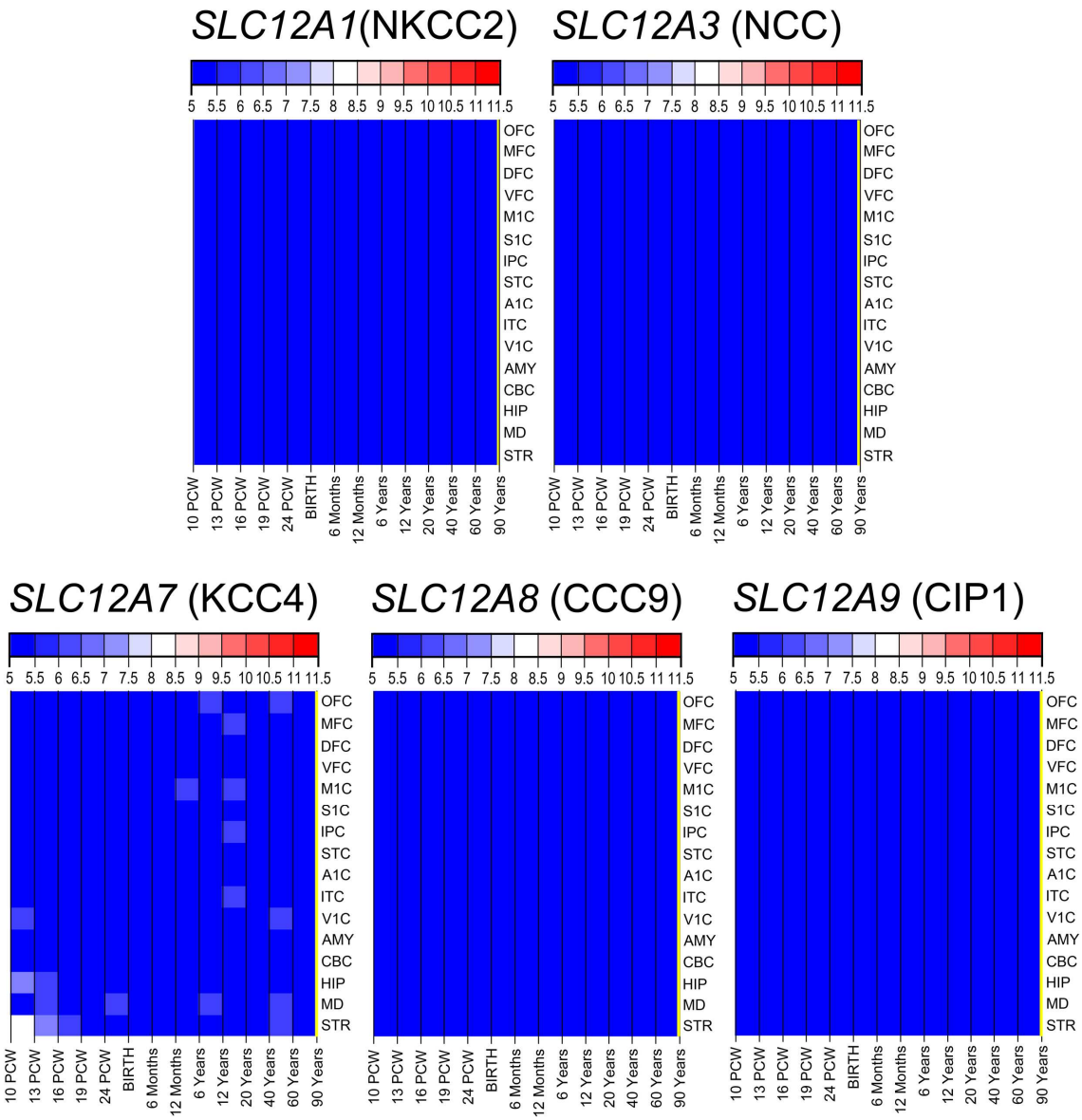

Supplementary Figure 2. **Double-labeling immunocytochemistry for KCC2 and NeuN.**

Positive NeuN (dark nucleus) and KCC2 (brown cell bodies) cells can be observed in all brain regions. After 25 PCW numerous double stained neurons can be observed in the human brain. Images represent 33 PCW specimen with substantial number of KCC2 and NeuN positive cells. Antibodies used KCC2 (as described in the main text; 1:1000), NeuN – monoclonal mouse-anti-NeuN (1:500; Millipore Corporation, CA, USA) according to the standard protocol.

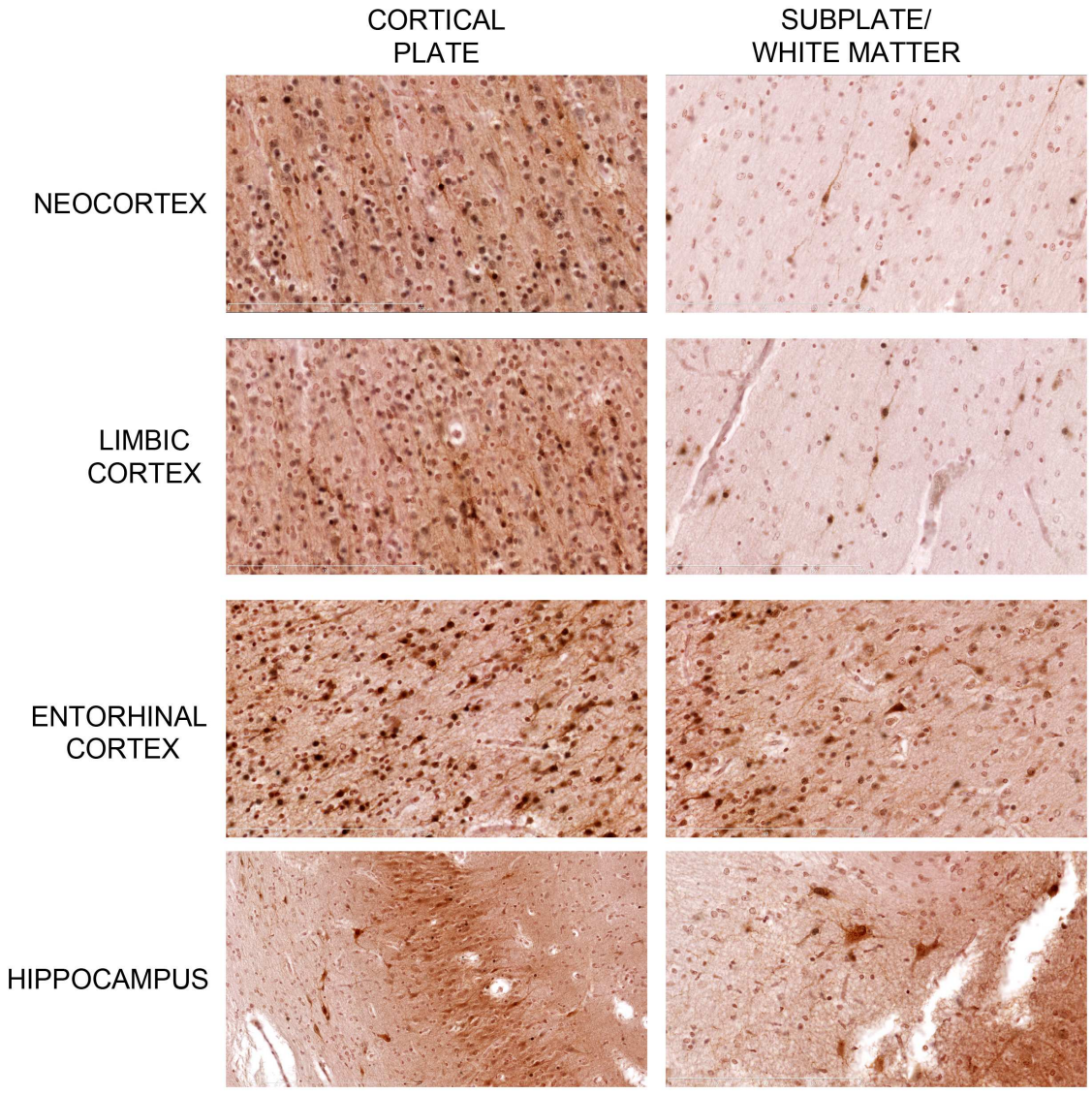

Supplementary Figure 3. **Developmental expression pattern of KCC2 immunoreactivity in the cingulate cortex.**

KCC2-ir was present in the cingulate cortex from 25 PCW onwards in both the cortical plate (A) and the subplate (E). KCC2-ir neurons at 33 PCW (B, F), 40 PCW (C, G) and 51 years (D, H). Note that KCC2-ir was present in the adult subcortical white matter interstitial neurons (H). Bar = 100 μm.

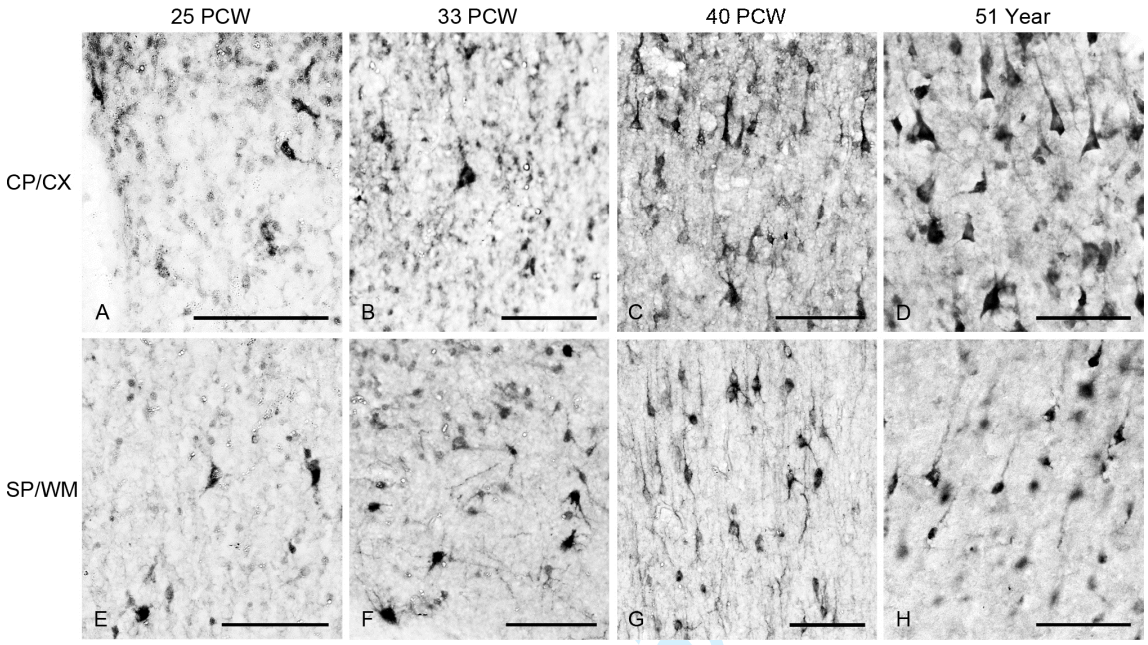

Supplementary Figure 4. **Developmental expression pattern of KCC2 immunoreactivity in the thalamus.**

Strong KCC2-ir in neuronal bodies and proximal dendritic shafts was observed in thalamus from 22 PCW onwards (A). Note that the basic pattern of KCC2-ir thalamic neurons (the reactivity of cell body and proximal dendrites) remains similar from midfetal period to the birth, i.e. at 25 PCW (B), 27 PCW (C), 33 PCW (D), 36 PCW (E) and 40 PCW (F). Bar = 100 μm.

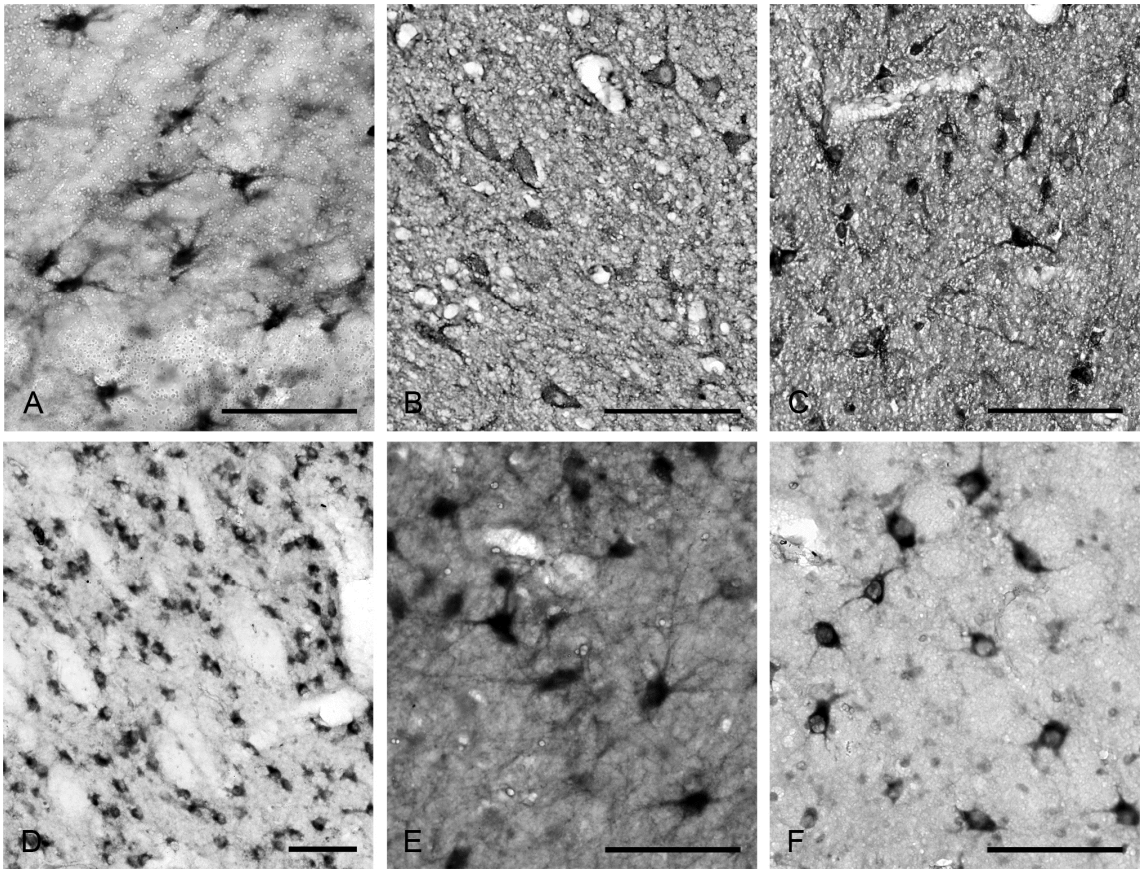

Supplementay Figure. 5. **Developmental expression pattern of KCC2 immunoreactivity in the basal ganglia.**

Neurons in the globus pallidus display strong KCC2-ir in their cell body and proximal dendritic shafts at 22 PCW (A). At 33 PCW (B) and 40 PCW (C), the KCC2-ir also extends into distal dendrites of pallidal neurons. KCC2-ir neurons were also observed at 40 PCW in the claustrum (D), nucleus caudatus (E) and putamen (F). Bar = 100 μm.

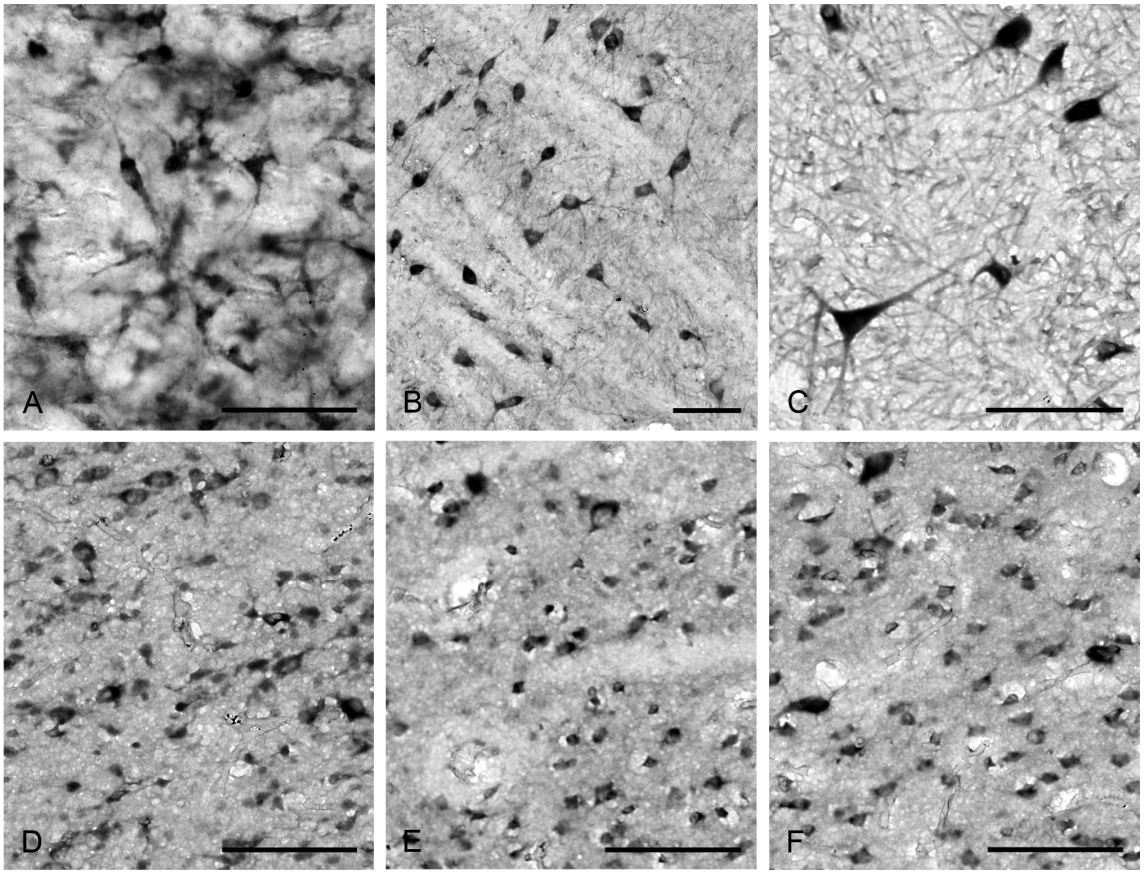

Supplementary table 1: Sixteen brain regions in which gene expression was analyzed, as previously defined (Kang et al. 2011).

OFC	Orbital prefrontal cortex
MFC	Medial prefrontal cortex
DFC	Dorsolateral prefrontal cortex
VFC	Ventrolateral prefrontal cortex
M1C	Primary motor cortex
S1C	Primary somatosensory cortex
IPC	Posterior inferior parietal cortex
STC	Superior temporal cortex
A1C	Primary auditory cortex
ITC	Inferior temporal cortex
V1C	Primary visual cortex
AMY	Amygdala
CBC	Cerebellar cortex
HIP	Hippocampus
MD	Mediodorsal nucleus of thalamus
STR	Striatum

Supplementary table 2: List of all brains analyzed by immunohistochemistry, with age and postmortem delay (PMD)

CODE	AGE	PMD
CF568	16 PCW	12 hours
CF588	18 PCW	2 hours
CD297	20 PCW	12 hours
S40/09	20 PCW	6 hours
CF599	22 PCW	24 hours
F89/09	22 PCW	6 hours
CD311	25 PCW	10 hours
CD312	25 PCW	22 hours
CD293	26 PCW	19 hours
CF597	33 PCW	20 hours
CF551	35 PCW	24 hours
CF554	36 PCW	18 hours
CF587	40 PCW	5 hours
CD289	3 months	6 hours
CD277	13 months	15 hours
CD255	6.5 years	16 hours
C0369	51 years	22 hours

Supplementary table 3: Data matrix representing log2 transformed values of ***SLC12A1*** (encoding for NKCC2) in different regions at different developmental periods. White cells represent samples where the gene is expressed, while gray cells represent samples considered not expressed (cutoff value of 5.5 was used to determine expression status).

	3	4	5	6	7	8	9	10	11	12	13	14	15
OFC	3.7554	3.71157	3.6237	3.64045	3.61539	3.70429	3.74229	3.72725	3.79393	3.79794	3.80321	3.9153	3.73844
MFC	3.78655	3.69302	3.57746	3.68104	3.69536	3.7218	3.70494	3.74436	3.92492	3.86411	3.84206	3.80029	3.85507
DFC	3.77996	3.70649	3.63396	3.68341	3.62418	3.63298	3.71051	3.72626	3.85803	3.76151	3.85101	3.95333	3.73338
VFC	3.73734	3.746	3.59732	3.63911	3.68238	3.74562	3.68343	3.6544	3.90663	3.84855	3.8893	3.84639	3.78022
M1C	3.73788	3.72914	3.65156	3.65913	3.65985	3.71064	3.84379	3.8244	4.0547	3.77279	3.87838	4.05997	3.81677
S1C	3.69877	3.67827	3.72934	3.64711	3.63535	3.76723	3.8628	3.82844	4.08672	3.76677	3.85422	3.93655	3.82271
IPC	3.78865	3.72167	3.63678	3.66921	3.66897	3.72562	3.85593	3.73666	3.69766	3.8291	3.84449	3.91397	3.77197
STC	3.77636	3.82355	3.72252	3.65769	3.62176	3.60767	3.72803	3.76043	3.66445	3.76297	3.87801	3.9281	3.77017
A1C	3.78966	3.75578	3.66014	3.68811	3.6388	3.66659	3.70266	3.70111	3.88334	3.82854	3.85696	3.83669	3.78654
ITC	3.76307	3.82921	3.67105	3.62928	3.63029	3.69205	3.74063	3.80326	3.91603	3.80272	3.85575	3.97984	3.74513
V1C	3.74097	3.73909	3.71251	3.58405	3.68984	3.71942	3.70921	3.6648	3.78961	3.84116	3.80851	3.80713	3.79307
AMY	3.724	3.69122	3.61795	3.61336	3.65236	3.70405	3.85902	3.99338	3.90645	3.95074	3.82181	3.90172	3.86433
CBC	3.71091	3.63967	3.53672	3.61645	3.66743	3.72984	3.69978	3.62961	3.86875	3.77761	3.83377	4.0154	3.85626
HIP	3.6822	3.64451	3.66231	3.69538	3.77663	3.69331	3.80254	3.69024	3.79769	3.77855	3.85553	3.81931	3.82474
MD	3.69095	3.7529	3.75435	3.66024	3.83731	3.7968	3.89286	3.69781	3.72015	3.98428	3.80886	3.86419	3.79869
STR	3.75971	3.69356	3.70204	3.65572	3.68101	3.65385	3.81971	3.96005	3.8829	3.79879	3.88082	3.835	3.88226

Supplementary table 4: Data matrix representing log2 transformed values of ***SLC12A3*** (encoding for NCC) in different regions at different developmental periods. White cells represent samples where the gene is expressed, while gray cells represent samples considered not expressed (cutoff value of 5.5 was used to determine expression status).

	3	4	5	6	7	8	9	10	11	12	13	14	15
OFC	4.14593	4.11023	4.22177	4.03894	4.05362	4.09955	4.17289	4.11835	3.95334	4.01316	4.0657	4.1022	3.99122
MFC	4.28329	4.18948	4.0633	4.14478	4.03062	4.10801	4.18099	4.02186	4.23323	3.98958	4.13843	4.14928	3.98565
DFC	4.22414	4.24387	3.95382	4.14723	3.9936	4.04611	4.26391	4.0763	3.95955	4.00314	4.17724	4.01711	4.05923
VFC	4.22779	4.28705	4.03974	4.10276	4.09443	4.11269	4.13085	3.98099	4.03346	4.05479	4.12213	4.01159	4.13431
M1C	4.23383	4.33817	4.38108	4.20305	4.15169	4.03601	4.10717	4.23011	4.05592	4.02017	3.98789	4.03056	4.04902
S1C	4.29692	4.28026	4.21521	4.12609	3.99492	4.09397	4.21718	3.87898	4.21362	4.01362	4.00312	4.04607	4.1718
IPC	4.20187	4.15908	4.12078	4.06064	4.11538	4.09385	4.51337	3.93488	3.97471	4.06198	4.0084	4.07418	4.03087
STC	4.29718	4.4455	3.97831	4.13007	4.12705	4.01311	4.21663	3.93061	3.98794	3.9915	4.0827	4.07706	4.02238
A1C	4.18022	4.1423	4.15278	4.20996	4.08015	3.94813	4.03737	3.98845	4.10801	4.11077	4.11475	4.0321	4.03845
ITC	4.37156	4.32748	4.23502	4.10206	4.15635	4.07169	4.31957	3.98391	3.96494	4.1381	4.04337	4.15544	3.92826
V1C	4.24462	4.16284	4.13946	4.09824	3.99353	4.08095	4.22961	4.08044	4.1781	4.02819	3.98274	3.98285	4.07402
AMY	4.11132	4.24669	4.16137	4.06518	4.02743	4.16986	4.18077	4.08129	4.07705	4.26414	4.06382	4.14456	4.04879
CBC	4.05022	4.16486	3.89298	4.06743	4.20967	4.1773	4.12626	4.16641	4.20365	4.40455	4.10864	3.95627	3.96465
HIP	4.20355	4.30764	4.04472	4.14025	3.97205	4.0942	4.05084	3.89053	4.18148	3.93799	4.047	3.98312	4.08271
MD	4.21328	4.26972	3.97973	4.10437	4.31198	4.20349	4.35935	4.13262	4.13448	4.29567	3.94449	4.07272	4.12587
STR	4.22788	4.23848	4.0502	4.03303	4.16922	4.00419	4.30387	4.1521	4.03387	4.14527	4.02067	3.97748	4.2425

Supplementary table 5: Data matrix representing log2 transformed values of ***SLC12A7*** (encoding for KCC4) in different regions at different developmental periods. White cells represent samples where the gene is expressed, while gray cells represent samples considered not expressed (cutoff value of 5.5 was used to determine expression status).

	3	4	5	6	7	8	9	10	11	12	13	14	15
OFC	5.01312	4.83304	4.58853	4.42653	4.94365	4.8735	4.99554	5.1244	5.52543	5.36269	5.0838	5.50416	5.08369
MFC	5.14246	5.25735	5.06023	4.45202	5.14349	5.11059	4.86963	5.25774	5.0769	5.59082	5.04929	5.03459	4.98822
DFC	4.96743	4.61892	4.52869	4.36029	5.13367	4.90375	5.05597	5.47466	5.25387	5.37184	5.1387	5.00693	5.05244
VFC	4.89715	4.50368	4.67298	4.42235	4.62457	4.76289	4.72238	5.40846	5.36714	5.44796	5.22097	5.46339	4.94269
M1C	4.82361	4.56573	5.27709	4.58373	4.79145	5.1259	4.5993	5.5738	5.20757	5.55379	5.39184	5.11931	5.21084
S1C	4.79227	4.76485	5.18942	4.5755	4.58659	5.0581	4.87519	5.28467	4.77283	5.42813	5.15193	5.36818	5.12283
IPC	4.82361	4.76838	4.52746	4.26569	5.04124	4.83721	5.33824	5.43892	5.25157	5.75165	5.25647	5.19252	5.18255
STC	4.90086	4.67347	4.8131	4.2636	4.91681	4.84273	5.06478	5.33738	5.07068	5.36383	5.22282	5.22721	5.23883
A1C	4.80132	4.75296	4.25659	4.1971	4.49646	5.11223	5.19978	5.41068	4.72116	5.46202	5.27812	5.07403	5.1023
ITC	4.87265	4.71889	5.0214	4.39129	4.87734	4.82009	4.7914	5.44335	5.13042	5.58349	5.36536	5.45796	5.23049
V1C	5.9065	5.43345	4.70502	4.52453	4.61595	5.26991	5.06244	5.234	5.08155	5.15317	5.1934	5.53567	5.26265
AMY	5.29324	5.4763	5.26783	4.77069	4.96718	5.06313	4.77778	4.97413	4.89312	4.95084	4.89073	5.23478	4.78721
CBC	5.42222	5.24113	4.92769	5.01765	5.10716	4.78074	4.68047	4.53764	4.52942	4.92181	4.98654	4.53593	4.82662
HIP	6.00811	5.54762	5.24371	4.88189	5.21033	5.19466	5.46604	5.26712	5.11654	5.10477	5.3029	5.06462	5.45363
MD	5.49497	5.62514	5.02202	4.82226	5.63542	5.03878	5.00829	5.48768	5.58771	5.11771	5.28904	5.71685	5.20404
STR	7.34851	6.42964	5.86598	5.12657	5.3078	5.22574	5.05162	5.17524	4.89655	5.24264	5.23581	5.71376	5.14898

Supplementary table 6: Data matrix representing log2 transformed values of ***SLC12A8*** (encoding for CCC9) in different regions at different developmental periods. White cells represent samples where the gene is expressed, while gray cells represent samples considered not expressed (cutoff value of 5.5 was used to determine expression status).

	3	4	5	6	7	8	9	10	11	12	13	14	15
OFC	4.82804	4.71403	4.74762	4.97741	4.97768	4.88635	4.95152	4.45034	4.66731	4.74898	4.76535	4.71845	4.708
MFC	4.92081	4.7354	4.81373	4.95744	4.63042	4.83566	4.99056	4.63858	4.5854	4.76656	4.81667	4.92713	4.7737
DFC	4.73183	4.64135	4.98465	4.94244	4.8125	4.94841	4.81236	4.74416	4.86853	4.78532	4.9343	4.79685	4.98179
VFC	4.88625	4.72274	4.98627	5.0842	4.67607	4.41639	4.77223	4.61985	4.76342	4.79839	4.99418	4.86439	4.9255
M1C	4.70601	4.82163	5.12767	4.82481	4.50859	4.73276	4.8971	4.48117	4.99984	4.88521	4.81076	4.79811	4.74949
S1C	4.8016	4.84579	4.91014	4.93418	4.82228	4.86482	4.74848	4.58432	4.52162	4.73945	4.8663	4.68848	4.79002
IPC	4.88683	4.84518	4.92315	5.03947	4.62046	4.78028	5.24873	4.86173	4.80304	4.85715	4.77689	4.90375	4.64303
STC	4.7957	4.78308	5.22617	4.96171	4.69168	4.61233	4.78004	4.61872	4.42717	4.64913	4.85131	4.67916	4.67423
A1C	4.89682	4.73827	5.02378	4.9293	4.82008	4.86072	4.83761	4.88039	4.86019	4.70489	4.75433	4.79806	5.01252
ITC	4.90641	4.86361	5.04003	4.74132	4.72954	4.58012	4.67188	4.61977	4.64289	4.84366	4.76959	4.60856	4.82449
V1C	4.74097	4.7999	5.03571	4.93177	4.57165	4.70337	4.52546	4.70629	4.57156	4.73241	4.89358	4.88245	4.85755
AMY	4.79526	4.83927	4.90483	4.93252	4.67914	4.89672	4.81206	4.59935	4.80312	4.72848	4.85463	4.68255	4.90312
CBC	4.72495	4.63608	4.93242	4.93752	5.02766	5.16045	4.8625	4.95089	4.89093	5.02418	4.81277	4.95163	4.70545
HIP	4.6617	4.73387	4.90468	4.9213	4.58345	4.92794	4.90347	4.77291	5.09777	4.77784	4.87989	4.77065	4.83011
MD	4.65631	4.66013	4.97086	4.90941	4.84987	4.92616	4.75411	4.8804	4.621	4.92166	4.94893	4.7306	4.8188
STR	4.83591	4.68029	4.93337	4.84742	4.5442	4.78138	4.93519	4.88475	4.61684	4.88115	5.01395	4.91473	4.96945

Supplementary table 7: Data matrix representing log2 transformed values of ***SLC12A9*** (encoding for CIP1) in different regions at different developmental periods. White cells represent samples where the gene is expressed, while gray cells represent samples considered not expressed (cutoff value of 5.5 was used to determine expression status).

	3	4	5	6	7	8	9	10	11	12	13	14	15
OFC	4.19876	4.17324	4.14132	4.24167	4.4033	4.63225	4.61989	4.63439	4.91137	5.12896	4.84624	4.93742	4.77963
MFC	4.18238	4.25697	4.32191	4.13067	4.32838	4.81769	4.98116	4.63249	4.69202	5.34889	5.03806	4.6875	4.88302
DFC	4.28111	4.22814	4.25999	4.15437	4.33645	4.9698	4.87477	4.51303	5.05866	5.21902	4.85438	4.99836	5.00644
VFC	4.13969	4.13199	4.13683	4.12003	4.44417	4.87552	4.88938	4.76236	4.85277	5.1879	4.7396	4.97656	4.61496
M1C	4.29611	4.33276	3.94507	4.20988	4.23975	4.64797	5.13722	4.56474	4.99483	4.94674	4.73852	4.88549	4.75968
S1C	4.22599	4.28793	3.93738	4.23975	4.44302	5.04722	4.81349	4.69148	4.96144	5.0521	4.93318	4.92417	4.68504
IPC	4.2177	4.29318	4.15675	4.25949	4.4688	4.61938	5.15696	4.63471	4.60393	5.1853	4.85158	4.82906	4.84113
STC	4.18785	4.15449	4.13139	4.18526	4.26893	4.80839	4.88947	4.8506	4.5647	4.95123	4.86869	5.10557	4.75967
A1C	4.06362	4.20535	4.11599	4.11712	4.26184	4.69834	4.75524	4.88093	4.63183	5.08492	4.80146	4.97903	4.81853
ITC	4.04713	4.14451	4.23768	4.16277	4.38099	4.63729	4.76838	4.70614	4.59456	5.02369	4.84163	4.67236	4.89908
V1C	4.20883	4.29117	4.21019	4.21953	4.48434	4.66361	5.10563	4.88723	4.88139	5.15105	5.07843	5.25533	5.06359
AMY	4.14996	4.18556	4.42459	4.10098	4.39992	4.43724	4.77534	4.82626	4.50586	4.83263	4.98134	4.92692	4.89321
CBC	4.11495	4.08187	4.2835	4.29244	4.41783	4.64621	4.21324	3.97299	4.06578	3.97619	4.05931	4.48166	4.11096
HIP	4.37767	4.56109	4.20689	4.38738	4.56476	4.76627	4.98612	4.81905	4.83291	4.65995	5.2018	4.97336	5.12927
MD	4.35634	4.17897	4.37391	4.66305	4.47493	4.53583	4.94187	4.543	4.53672	4.65384	4.49768	4.62512	4.54796
STR	4.6088	4.298	4.9793	5.19028	4.6016	5.11354	5.2274	5.26197	5.21671	5.09192	5.04082	5.25116	5.08675

Supplementary table 8: Data matrix representing log2 transformed values of ***SLC12A2*** (encoding for NKCC1) in different regions at different developmental periods. White cells represent samples where the gene is expressed, while gray cells represent samples considered not expressed (cutoff value of 5.5 was used to determine expression status).

	3	4	5	6	7	8	9	10	11	12	13	14	15
OFC	6.98535	6.98629	7.60412	7.94765	7.16327	7.68799	8.87072	8.33796	9.45084	8.33358	8.71252	8.71916	8.74816
MFC	6.39635	6.61482	7.282	7.80283	6.35986	7.29303	8.36417	8.37362	8.81177	8.20485	8.47291	8.87784	7.75838
DFC	6.83813	6.37018	7.28087	7.64904	6.98979	7.66483	8.186	8.54093	7.9447	8.50575	8.86764	7.86239	8.50687
VFC	7.18997	6.75843	8.0992	7.74827	6.60968	7.3938	8.55099	8.98336	8.73958	8.82013	9.05185	8.81476	8.49023
M1C	6.73473	6.64061	6.60012	7.42586	6.70186	7.92329	8.31948	8.76354	8.94145	9.09611	9.02499	7.97869	8.88048
S1C	6.94788	6.30039	6.21409	7.09893	6.23241	7.35674	7.9895	8.30369	8.63348	8.75079	8.84372	8.7168	8.24488
IPC	6.72878	6.44794	6.36113	6.96242	6.57446	7.97589	7.36539	8.01132	9.26853	8.63448	8.61976	8.32144	8.25554
STC	6.67399	6.22654	6.8506	6.84729	6.48133	7.72307	7.75612	7.89913	8.20631	8.28193	8.79241	7.69904	7.84486
A1C	6.90573	6.88014	6.45799	6.66443	6.69879	7.99041	7.80742	7.93724	8.70793	8.76843	9.18719	8.21652	8.37484
ITC	6.7634	6.38421	6.51981	6.2778	6.07825	6.48987	7.53334	8.23302	8.19902	8.4771	8.24559	7.74971	7.65709
V1C	6.59038	6.41338	7.14135	7.28846	6.80953	7.7155	7.62905	8.34994	9.20024	8.07754	8.97771	8.28656	8.25825
AMY	7.35276	7.01901	6.48314	7.15662	6.3087	7.17525	8.33345	7.6864	8.83261	8.86745	8.7813	7.40085	7.92558
CBC	6.68149	6.25075	7.40906	6.78993	6.21315	8.40818	8.19922	8.51948	8.62549	8.68883	8.07365	7.20479	7.63316
HIP	6.79653	6.21306	6.451	6.37122	6.33515	7.13354	8.35664	9.05542	8.47839	8.67785	8.70929	8.35128	7.98782
MD	7.80973	7.82026	7.79034	7.82079	6.57676	8.43324	8.46109	8.87625	8.95491	9.24688	9.25685	9.3618	8.5964
STR	6.49716	6.90962	6.21043	6.28767	6.35917	8.06653	7.99464	8.85336	7.49248	8.72337	9.43302	8.81863	8.15178

Supplementary table 9: Data matrix representing log2 transformed values of ***SLC12A6*** (encoding for KCC3) in different regions at different developmental periods. White cells represent samples where the gene is expressed, while gray cells represent samples considered not expressed (cutoff value of 5.5 was used to determine expression status).

	3	4	5	6	7	8	9	10	11	12	13	14	15
OFC	9.10494	8.83637	8.58099	8.09215	8.00167	7.44032	7.35013	6.76722	7.92779	7.8034	8.08972	7.8361	7.81557
MFC	9.19531	8.68236	8.60026	8.37448	7.82983	7.34802	7.5225	6.87304	7.92775	7.5781	7.84869	7.41301	7.77327
DFC	9.04188	9.04714	8.51788	8.23626	8.03928	7.90955	7.42611	7.17331	7.85003	7.94623	8.0242	7.46093	7.65113
VFC	9.04656	8.952	8.37313	8.27394	7.91546	7.51361	7.4722	7.55572	8.0267	7.93074	8.33458	7.85752	7.46519
M1C	9.1726	9.25624	8.56947	8.40021	7.89262	7.75501	7.60874	7.31396	7.23614	8.03854	8.387	7.43227	8.00421
S1C	9.1198	9.13606	8.52005	8.54189	7.97147	6.88203	7.20138	7.63422	7.59929	8.06209	8.03851	8.0328	7.79505
IPC	8.94473	9.13108	8.47428	8.45467	8.07767	7.77916	7.21219	7.12575	8.08741	7.94659	8.22415	7.57099	7.65202
STC	9.0032	8.45871	8.30859	8.49798	8.09271	7.45334	7.12537	7.03566	7.14565	7.58551	8.02651	7.71739	7.70659
A1C	8.81662	8.68002	8.21586	8.13332	8.37467	7.52016	7.95469	7.27628	7.80866	7.60076	8.28657	7.74594	7.77122
ITC	8.58714	8.63461	8.39149	8.20257	8.08921	7.22651	7.07551	6.59858	7.78295	8.04763	8.10832	7.22492	7.64964
V1C	9.16136	8.87762	8.4876	8.60625	7.6683	7.93373	7.43782	7.28817	8.29504	7.41911	8.28886	7.81184	7.36302
AMY	8.37031	8.75509	8.31573	8.61388	7.50713	7.61663	7.93381	6.86261	8.07289	7.52053	8.07244	7.1855	7.10876
CBC	9.01103	8.74308	8.1904	7.84976	7.26902	6.93967	7.20925	7.03898	7.82315	7.36702	7.85163	6.86622	6.98123
HIP	8.35909	8.17469	8.41604	8.01098	7.46448	7.56441	7.19353	7.41988	7.83939	7.77465	7.71626	7.16613	6.91561
MD	8.33061	8.09533	8.2209	7.75206	7.39755	7.09641	7.08195	7.12008	7.92055	7.38381	7.72242	7.62887	7.03711
STR	8.75959	8.68762	8.84648	8.58988	7.57516	7.18016	8.03948	7.31224	7.19592	7.91723	8.21575	7.63653	7.21742

Supplementary table 10: Data matrix representing log2 transformed values of ***SLC12A4*** (encoding for KCC1) in different regions at different developmental periods. White cells represent samples where the gene is expressed, while gray cells represent samples considered not expressed (cutoff value of 5.5 was used to determine expression status).

	3	4	5	6	7	8	9	10	11	12	13	14	15
OFC	4.43723	4.84044	4.58183	4.59162	4.96352	5.55146	5.35699	5.63969	5.32169	5.41471	5.15351	5.31624	5.08195
MFC	4.21519	4.93892	4.75664	4.45181	5.22482	5.60962	5.2186	5.91506	5.0707	5.64455	5.13615	5.33158	5.46074
DFC	4.39099	4.54323	4.57473	4.35249	5.12312	5.31367	5.02216	5.72497	5.31427	5.31433	5.09131	5.09227	5.0697
VFC	4.29605	4.28554	4.41846	4.33857	5.05965	5.42977	5.16667	5.49201	5.15066	5.56751	5.15635	5.26296	5.39279
M1C	4.38549	4.25569	4.48415	4.47836	5.07446	5.39171	5.15678	5.76242	4.94004	5.48492	4.91768	5.04168	5.28489
S1C	4.26077	4.17488	4.65996	4.44521	5.1399	5.40375	4.9951	5.49241	4.94413	5.3589	5.03865	5.16826	5.21
IPC	4.21311	4.31281	4.08297	4.35145	5.32062	5.32538	4.96102	5.43829	5.03198	5.39284	5.00946	5.0924	5.40842
STC	4.33248	4.39752	4.52396	4.40762	4.8403	5.33632	5.04212	5.15221	5.0888	5.20432	4.95357	5.04956	5.06319
A1C	4.26888	4.4571	4.10593	4.33415	4.89684	5.52541	4.98332	5.74122	5.22026	5.38497	5.11913	5.08978	4.97056
ITC	4.43918	4.55371	4.75601	4.49667	5.1538	5.46411	5.25635	5.79963	5.22731	5.42705	5.10076	5.21773	5.29584
V1C	4.64992	4.76782	4.69826	4.35825	4.93019	5.62854	5.08916	5.27468	5.10712	5.71838	4.9271	5.01295	5.14085
AMY	5.0923	5.50973	5.18684	5.07585	5.46026	5.47885	5.49911	5.43409	5.36766	5.46951	5.27999	5.40993	4.93025
CBC	5.67487	5.84785	6.77145	7.10479	6.83319	6.89119	6.03416	6.43441	6.57643	6.22777	5.7431	5.52013	5.91953
HIP	5.05789	5.39171	5.31997	5.10124	5.66531	5.90416	5.99572	5.58179	5.21144	5.74991	5.46293	5.38835	5.55425
MD	4.71475	4.88352	4.8775	5.08857	5.48981	5.97328	6.04725	5.7991	6.01833	5.99121	5.65399	6.06745	5.9883
STR	4.6854	5.0146	4.77463	5.13611	6.22134	5.99164	5.32236	5.36281	5.69435	5.66282	5.32151	5.58872	5.35589

Supplementary table 11: Data matrix representing log2 transformed values of ***SLC12A5*** (encoding for KCC2) in different regions at different developmental periods. White cells represent samples where the gene is expressed, while gray cells represent samples considered not expressed (cutoff value of 5.5 was used to determine expression status).

	3	4	5	6	7	8	9	10	11	12	13	14	15
OFC	4.5053	4.71418	4.8001	5.66918	6.96302	8.87889	8.98047	7.82262	9.37508	9.80537	9.68272	9.53576	9.58455
MFC	4.37181	4.60274	4.57775	5.68318	6.58366	9.08761	8.92819	8.16594	9.37828	9.1281	9.34644	9.01847	9.5783
DFC	4.4446	4.5834	4.82656	5.12368	7.14991	9.10092	9.13021	8.46023	9.63056	9.75089	9.59383	9.47026	9.6149
VFC	4.66229	4.84501	5.20782	5.95644	6.99045	8.81244	9.29108	8.86446	9.49876	9.7535	9.75921	9.58684	9.5945
M1C	4.8262	4.92092	5.52939	6.67414	7.33539	9.28139	9.59415	9.22906	9.19489	9.57476	9.79509	9.53261	9.94104
S1C	4.58287	4.92795	5.12113	6.46389	7.28482	8.96711	9.16126	8.71638	9.4184	9.71419	9.88503	9.69505	9.75413
IPC	4.38649	4.82228	5.20193	5.56942	7.06277	9.0722	9.1445	8.65192	8.89316	9.84682	9.9129	9.53474	9.86231
STC	4.39806	4.46107	4.92584	5.73187	6.92797	8.95281	9.06021	8.49508	9.15411	9.44732	9.80087	9.53617	9.88072
A1C	4.59313	4.84197	4.80783	5.65239	6.88574	9.21657	9.69608	8.34762	9.49567	9.42701	9.85287	9.82834	9.80544
ITC	4.63073	4.41793	5.18336	5.95036	6.98881	8.66713	8.86184	8.88335	9.44343	9.5511	9.61948	9.51339	9.63107
V1C	4.19365	4.1749	4.37473	5.03174	6.9706	9.35499	9.18778	8.95956	10.0851	9.29432	10.0639	10.2027	9.51023
AMY	6.00117	5.75655	6.0188	5.98613	6.45575	8.81714	9.34379	8.34858	9.61514	9.37001	9.17763	7.59156	8.69257
CBC	6.16913	5.69862	6.20509	5.47125	5.88129	8.17855	9.2319	9.43178	9.70835	10.1541	10.1123	9.69621	9.36619
HIP	4.07	4.16168	5.64545	6.03194	5.86655	8.88693	9.09826	9.01589	9.45733	9.22645	9.16488	9.10873	9.15447
MD	7.41907	7.92677	8.25428	8.40721	7.86815	9.4631	9.30732	9.32486	9.47366	9.69207	9.60167	9.48179	9.17847
STR	5.46498	5.25956	6.98657	6.5452	4.42198	8.98661	9.59023	8.45992	8.8401	9.63167	9.31692	9.14059	9.31565

Supplementary table 12: Data matrix representing log2 transformed values of ***NTRK2*** (encoding for TrkB) in different regions at different developmental periods. White cells represent samples where the gene is expressed, while gray cells represent samples considered not expressed (cutoff value of 5.5 was used to determine expression status).

Area	3	4	5	6	7	8	9	10	11	12	13	14	15
OFC	8.24209	8.5698	9.1499	10.2156	10.639	11.2415	11.3328	10.8392	11.6144	11.4602	11.4002	11.3161	11.45
MFC	8.71701	8.7412	8.51099	9.63908	10.2051	11.1163	11.4094	11.0582	11.5599	11.3274	11.394	11.2027	11.3558
DFC	8.146	8.17345	8.5908	9.84147	10.4999	11.2177	11.3602	11.3316	11.4401	11.2064	11.1293	11.4728	11.4
VFC	8.61339	9.03061	9.4454	10.0744	10.4134	11.2314	11.3824	11.0933	11.7454	11.3835	11.1748	11.3619	11.2874
M1C	9.13792	8.86381	9.62661	10.0108	10.1514	11.3298	11.2389	11.1333	11.4286	11.2185	11.125	11.2642	11.2634
S1C	9.71042	9.40595	10.1783	10.1345	10.6891	11.0749	11.3501	11.1139	11.5092	11.304	11.1851	11.1879	11.2848
IPC	10.1107	10.3135	10.1834	10.2417	10.4337	11.2421	11.1673	11.5031	11.6864	11.3216	11.1987	11.5005	11.436
STC	10.3896	10.5341	9.90781	10.4608	10.4938	11.4684	11.4405	11.1972	11.712	11.2776	11.1857	11.2664	11.4982
A1C	10.322	10.3269	10.1887	10.4828	10.574	11.3685	11.2886	11.3481	11.5976	11.1454	11.2296	11.2145	11.3509
ITC	10.2991	10.3435	10.009	10.2169	10.13	11.3834	11.3867	11.0689	11.6135	11.3378	11.3957	11.4272	11.4089
V1C	9.08563	9.321	10.2275	10.5748	10.6994	11.3945	11.0732	11.4289	11.4364	11.2197	11.0761	10.8946	10.8405
AMY	10.4007	9.99086	9.86795	10.3523	10.8343	10.8414	11.1371	10.9387	11.1244	10.8869	11.0025	10.5898	10.8707
CBC	9.65271	9.91398	10.4822	10.106	9.0022	9.73849	10.2638	10.3741	10.7115	10.4205	10.2939	9.93641	10.9619
HIP	8.79377	8.64794	9.75119	10.2812	10.1463	10.9855	10.9232	10.7988	11.1548	10.7976	10.7747	11.1831	10.6643
MD	10.1736	9.6263	10.0147	10.1391	10.8663	10.9257	11.2656	11.0112	10.9534	10.8831	10.9796	10.8592	11.0104
STR	10.0183	10.1201	10.1711	10.1816	10.2038	10.506	11.375	10.7095	11.0426	10.6713	10.6434	10.7337	10.6492

Supplementary table 13: Data matrix representing log2 transformed values of ***ATP1A1*** (encoding for Na-K ATPase α1) in different regions at different developmental periods. White cells represent samples where the gene is expressed, while gray cells represent samples considered not expressed (cutoff value of 5.5 was used to determine expression status).

Area	3	4	5	6	7	8	9	10	11	12	13	14	15
OFC	7.00198	7.03124	6.95638	7.1283	7.49084	8.07409	7.99485	7.30009	7.88273	8.25904	8.29566	8.11393	8.75434
MFC	7.17649	7.54224	6.95086	7.30751	7.10628	7.772	7.60367	7.56471	8.69318	7.79339	7.59911	7.46094	8.23558
DFC	7.16253	7.18768	6.46585	7.06783	7.48925	7.91897	7.93868	7.18113	8.08155	8.0812	8.01009	7.45777	8.06507
VFC	7.03945	7.06472	7.2178	7.16934	7.20461	7.93516	7.81513	8.00577	7.97855	8.07136	8.6497	8.20569	8.98227
M1C	7.15448	7.28157	7.34782	7.68914	7.4897	7.99063	7.70249	7.52606	8.2504	8.57677	8.90541	7.94934	8.84649
S1C	7.37006	6.97985	6.71166	7.59668	7.5233	7.34818	7.82859	7.90203	8.56285	8.29568	8.72878	8.2533	9.09016
IPC	6.80457	7.08725	7.44398	7.2487	7.08775	8.34574	7.65922	7.72188	8.23602	8.32366	8.43285	7.9209	8.65371
STC	6.76953	6.64044	6.75583	7.35762	7.39587	7.33633	7.4617	7.53276	7.75761	8.07623	8.33424	8.21085	8.49292
A1C	6.86316	6.74342	7.13443	7.25406	7.48828	7.76357	7.70555	7.79558	8.66361	8.22681	8.73277	8.06042	8.58255
ITC	6.39708	5.98115	6.61488	7.00681	6.80044	7.5111	7.705	7.28597	7.79023	7.71065	8.07414	7.41589	8.07929
V1C	6.72648	6.92457	6.64264	7.54321	7.65766	8.08741	8.49089	7.5753	9.09709	7.78278	8.67905	9.03846	8.54828
AMY	6.53638	6.5486	6.87414	6.32804	6.38894	7.40199	7.48648	6.64793	7.39397	7.32002	7.64357	7.44553	7.15492
CBC	6.91087	6.60172	6.70769	6.54044	7.96941	8.82969	9.36094	9.51959	8.7831	9.41226	9.15007	7.91306	8.12102
HIP	6.24366	6.33912	6.8756	7.0808	5.98431	7.13438	7.17451	7.50392	7.85385	7.52607	7.60429	7.72929	8.36915
MD	6.7367	6.70563	6.75925	6.92265	6.85156	7.42164	7.54092	8.18945	7.49513	7.53205	7.44823	7.45142	7.52329
STR	6.79735	6.5484	6.97591	7.16713	6.37485	7.6593	7.46412	7.3841	7.50975	8.08257	7.97796	7.55329	7.91067

Supplementary table 14: Data matrix representing log2 transformed values of ***ATP1A2*** (encoding for Na-K ATPase α2) in different regions at different developmental periods. White cells represent samples where the gene is expressed, while gray cells represent samples considered not expressed (cutoff value of 5.5 was used to determine expression status).

Area	3	4	5	6	7	8	9	10	11	12	13	14	15
OFC	6.37493	7.28397	6.66562	7.47304	9.05685	11.1255	10.7162	11.8623	10.7473	10.9836	10.5069	10.3862	10.8482
MFC	5.52994	7.03891	7.62275	7.26543	9.50743	11.2676	10.6906	11.885	11.1055	11.1811	10.538	10.6214	10.9198
DFC	5.54322	5.53076	6.91205	6.51581	9.15599	10.8874	10.501	11.6816	10.9301	10.9063	10.4195	10.3246	10.8203
VFC	4.94142	4.6647	6.62299	7.0895	9.14382	10.8747	10.4567	11.3028	10.6189	11.1429	10.2399	10.3333	10.6558
M1C	4.82689	4.83025	6.55572	7.44802	9.35386	11.2727	10.0981	11.6551	10.404	11.0944	10.3115	10.7186	11.1031
S1C	4.85036	4.85975	6.89012	7.27124	9.16324	11.011	10.0796	11.8038	10.3681	11.3528	10.2338	10.6063	10.9237
IPC	4.66677	4.82615	5.94221	6.52825	8.8512	10.9791	10.061	11.7518	10.4981	11.14	10.1528	10.5024	11.0581
STC	4.8414	5.29278	6.7295	6.23711	8.64701	10.9243	10.4076	11.0898	10.7457	11.0687	10.357	10.368	10.9048
A1C	4.80866	5.45409	5.06276	6.48925	8.65581	11.1756	10.4468	11.1203	10.4976	11.2439	10.1699	10.4915	11.0998
ITC	5.1435	5.931	7.53028	7.26666	8.68428	10.9652	10.4848	11.6589	10.8939	11.0141	10.6175	10.5783	10.817
V1C	5.76207	6.41418	7.02641	7.07571	8.76764	11.1247	10.0892	11.7967	10.2861	10.9594	10.1958	10.1075	10.621
AMY	7.85479	8.22812	8.37066	9.50387	10.3106	11.2897	10.9824	11.2623	10.9565	10.9094	10.9652	11.0373	10.8345
CBC	8.45464	8.57833	9.84716	9.78522	8.98986	10.4827	10.1516	10.4311	10.2784	10.7226	9.83627	9.53847	10.9008
HIP	8.97498	9.25372	9.13197	9.49873	10.6861	11.5112	11.1188	11.2076	10.9231	11.3498	10.7155	10.8977	10.8416
MD	7.32479	7.33196	7.87335	9.50415	10.1706	11.4154	11.1933	11.4726	11.6039	11.1704	11.031	11.4431	11.3661
STR	5.97948	6.59547	8.27241	9.01657	10.6387	11.3108	10.9677	11.0484	10.5344	11.1091	11.131	11.0914	10.9273

Supplementary table 15: Data matrix representing log2 transformed values of ***ATP1A3*** (encoding for Na-K ATPase α3) in different regions at different developmental periods. White cells represent samples where the gene is expressed, while gray cells represent samples considered not expressed (cutoff value of 5.5 was used to determine expression status).

Area	3	4	5	6	7	8	9	10	11	12	13	14	15
OFC	6.67933	6.83735	6.29035	6.50093	7.12775	6.41564	6.1484	4.84302	5.02612	6.05004	5.94631	5.71091	5.9491
MFC	7.22345	7.32408	6.29181	6.37317	6.38128	6.48807	6.13416	5.52148	5.32458	6.09551	6.09003	5.78406	6.18842
DFC	6.97662	7.48635	6.71353	6.25862	6.96469	6.48079	6.1418	5.11326	5.70698	6.15261	6.02296	5.7863	5.71084
VFC	6.8996	7.16256	6.64509	6.62507	6.78342	6.33585	6.30533	5.37281	5.13605	6.36991	6.02669	5.70981	5.90064
M1C	7.13845	7.50059	7.33021	6.6956	6.68795	6.49505	5.86587	5.82927	5.86361	5.65564	6.4018	6.47569	6.26492
S1C	7.58804	7.234	7.02247	6.51658	6.89607	6.36296	6.26452	4.9397	5.11307	6.20935	6.44212	6.56405	6.06441
IPC	7.37799	7.27476	6.58231	6.55779	7.45849	6.18961	6.09309	4.89618	5.25668	6.1134	6.47434	5.60511	6.12831
STC	7.16553	7.08171	5.95421	6.51857	6.90165	6.13278	6.42119	4.99583	4.81209	5.96815	6.07272	5.98082	5.73637
A1C	6.92299	6.97706	5.96768	6.44074	6.88489	6.0804	6.42339	5.53972	5.81108	5.80231	6.28525	5.57671	6.04963
ITC	6.71239	7.02007	6.53804	6.35272	7.11662	6.74927	6.17377	5.58632	5.37496	5.79081	6.28109	5.37379	5.71132
V1C	7.86832	7.68219	6.00607	6.35616	6.38746	6.65271	6.23952	5.54498	6.0322	6.21221	6.4172	6.48367	5.98717
AMY	6.27535	6.57033	6.00106	5.89031	5.93269	6.38564	6.02046	5.70084	6.12111	5.76563	6.32481	5.18413	5.29933
CBC	6.83522	7.54859	6.2319	6.62743	7.73155	7.04634	6.65029	5.35776	5.26291	6.29684	6.524	5.84758	6.11973
HIP	6.3561	6.41598	6.03226	5.96859	5.8683	6.53501	6.01918	5.95092	6.65653	6.34312	6.61749	6.18779	6.38392
MD	6.32928	6.61426	7.01519	6.31259	6.26489	6.99756	7.11161	6.86028	6.59464	7.26405	7.13246	6.79363	6.27351
STR	6.82842	6.73576	6.10134	5.57036	5.36469	5.52801	5.57743	5.40497	5.22509	5.21706	5.43038	5.08329	5.16874

Supplementary table 16: Data matrix representing log2 transformed values of ***ATP1A4*** (encoding for Na-K ATPase α4) in different regions at different developmental periods. White cells represent samples where the gene is expressed, while gray cells represent samples considered not expressed (cutoff value of 5.5 was used to determine expression status).

Area	3	4	5	6	7	8	9	10	11	12	13	14	15
OFC	3.61326	3.60755	3.57554	3.64812	3.67249	3.59857	3.70414	3.7242	3.67166	3.71423	3.65763	3.75634	3.68176
MFC	3.62452	3.55595	3.59242	3.64306	3.66862	3.59929	3.69866	3.87273	3.55568	3.75121	3.63714	3.66879	3.59991
DFC	3.61503	3.64134	3.6387	3.6443	3.84911	3.69134	3.67952	3.70022	3.66289	3.62697	3.72773	3.66904	3.74138
VFC	3.59116	3.59611	3.6531	3.63769	3.67416	3.653	3.7812	3.61866	3.70256	3.62854	3.66234	3.58352	3.74935
M1C	3.63204	3.66243	3.65992	3.63984	3.70244	3.6124	3.81693	3.57508	3.70379	3.57594	3.66302	3.72959	3.63023
S1C	3.59494	3.71653	3.59913	3.62205	3.73515	3.68937	3.65763	3.68359	3.63359	3.65972	3.65209	3.64954	3.61547
IPC	3.73576	3.64411	3.63785	3.64887	3.6567	3.64962	3.76607	3.63547	3.58417	3.58656	3.60809	3.7475	3.74963
STC	3.57805	3.68168	3.65018	3.61289	3.67175	3.61812	3.80231	3.72339	3.71228	3.64541	3.71639	3.64449	3.62787
A1C	3.57632	3.65005	3.6534	3.69142	3.60259	3.60863	3.81455	3.73694	3.59261	3.6499	3.64428	3.71332	3.66734
ITC	3.6634	3.64993	3.65681	3.65041	3.64102	3.62179	3.73074	3.69708	3.69491	3.67775	3.66656	3.65525	3.64525
V1C	3.65343	3.74466	3.62597	3.64381	3.65597	3.69334	3.70911	3.74111	3.75202	3.6029	3.67065	3.63088	3.68248
AMY	3.65315	3.63502	3.58805	3.61738	3.84279	3.73899	3.64004	3.70763	3.64925	3.68879	3.69427	3.74383	3.73868
CBC	3.56872	3.56229	3.60766	3.64856	3.69899	3.57544	3.65587	3.54702	3.62069	3.69219	3.61141	3.61881	3.63487
HIP	3.61577	3.57553	3.63902	3.6423	3.7058	3.5861	3.7033	3.64448	3.67914	3.75676	3.66437	3.617	3.70904
MD	3.61331	3.69508	3.58793	3.66406	3.76575	3.72579	3.63179	3.79537	3.74525	3.61189	3.67474	3.69987	3.6896
STR	3.60149	3.67379	3.56502	3.59236	3.78666	3.70896	3.78903	3.70475	3.62308	3.61634	3.65156	3.71284	3.71602

Supplementary table 17: Data matrix representing log2 transformed values of ***ATP1B1*** (encoding for Na-K ATPase β1) in different regions at different developmental periods. White cells represent samples where the gene is expressed, while gray cells represent samples considered not expressed (cutoff value of 5.5 was used to determine expression status).

Area	3	4	5	6	7	8	9	10	11	12	13	14	15
OFC	8.05368	7.974	8.60149	8.88919	9.40524	10.0495	10.2853	9.07689	10.2249	10.4169	10.1902	10.2389	10.3584
MFC	8.21854	8.33066	8.28429	9.33013	9.00967	10.1757	10.1759	8.80725	10.1355	10.121	10.1042	10.0037	10.3034
DFC	8.06041	8.20403	8.3347	9.03438	9.27477	10.1573	10.2928	9.23244	9.71685	10.2496	10.1261	10.0363	10.3814
VFC	7.96744	8.13087	8.86523	9.29951	9.236	10.2207	10.3758	9.87602	10.1964	10.4597	10.244	10.1733	10.7973
M1C	7.97321	8.19569	8.70333	9.63045	9.25609	10.1554	10.2341	9.33725	10.3451	10.5997	10.4292	10.4679	10.6991
S1C	8.22248	8.14714	8.01431	9.78755	9.34451	10.1806	10.3475	9.00958	10.2234	10.5242	10.4963	10.6493	10.7608
IPC	8.04814	8.20868	8.71677	9.33541	9.36292	10.376	10	9.16744	10.6546	10.4453	10.3933	9.94411	10.4002
STC	8.07309	7.68753	8.64469	9.43145	9.6365	10.1217	10.1191	8.7945	9.99	10.2713	10.3112	10.2196	10.4526
A1C	8.016	7.81454	9.10992	9.54717	9.3959	10.1374	10.2281	9.433	10.3032	10.4925	10.5145	10.3715	10.6301
ITC	7.97855	7.9302	8.17468	9.15532	9.13998	10.1103	9.99053	8.56963	9.9754	9.97673	10.0966	9.99131	10.1473
V1C	7.6671	7.59259	8.25983	8.93873	9.22182	9.93749	10.1984	9.30471	10.633	10.7661	10.441	10.3023	10.3027
AMY	7.97845	8.102	8.27646	8.54958	8.93502	9.62199	9.89303	8.60795	10.3943	10.1708	9.69326	9.21528	10.0923
CBC	8.17191	7.83948	8.65718	7.42172	7.63645	9.23108	9.42539	8.95965	9.61669	10.0159	10.0637	9.51739	9.93814
HIP	7.99592	7.3653	8.51059	8.92058	7.33199	10.3238	9.85611	9.75193	10.7693	10.5241	10.4016	9.897	10.7133
MD	8.77802	8.744	9.35018	9.3182	9.62664	10.4676	10.5339	10.1351	11.1659	10.7804	10.7408	10.6571	10.4168
STR	7.62584	7.59082	8.11847	8.01578	7.6251	9.6711	9.38279	9.30682	9.62222	9.67762	9.88509	9.41022	9.53006

Supplementary table 18: Data matrix representing log2 transformed values of ***ATP1B2*** (encoding for Na-K ATPase β2) in different regions at different developmental periods. White cells represent samples where the gene is expressed, while gray cells represent samples considered not expressed (cutoff value of 5.5 was used to determine expression status).

Area	3	4	5	6	7	8	9	10	11	12	13	14	15
OFC	9.64346	9.84122	9.96167	10.3597	11.412	12.0526	11.6256	12.4088	11.1176	12.0144	11.4724	11.2262	11.6024
MFC	9.85731	9.6773	9.90841	10.5255	11.6095	11.9078	11.6127	12.5346	11.4327	12.2659	11.4998	11.48	11.8927
DFC	9.74393	10.0764	9.43983	10.2289	11.585	11.8622	11.358	12.4786	11.3255	12.0805	11.3888	11.4153	11.5761
VFC	9.6215	9.88664	9.68748	10.2716	11.4909	11.8273	11.6917	12.0584	11.366	12.2394	11.0584	11.0173	11.624
M1C	9.96874	9.95659	10.1314	10.7831	11.7308	12.2522	11.2985	12.3521	11.057	12.2721	11.0235	11.3532	11.7217
S1C	9.85622	9.82573	10.3421	10.5532	11.611	11.8728	11.0834	12.596	11.2311	12.3763	11.0849	11.3558	11.6377
IPC	9.74008	10.1354	9.86428	10.4565	11.6403	11.9833	11.3524	12.4603	11.3973	12.1848	10.9995	11.2761	11.6097
STC	9.89412	10.1335	9.51237	10.4895	11.4071	12.1342	11.4573	12.2263	11.4045	12.0172	11.2478	11.124	11.6119
A1C	9.70474	10.017	9.40503	10.376	11.5	12.0955	11.2869	12.4223	11.1743	12.2592	10.9023	11.2488	11.4827
ITC	9.60132	9.75787	9.93567	10.3752	11.2232	12.0688	11.6321	12.5865	11.7642	12.3665	11.6045	11.5601	11.6349
V1C	10.0726	10.21	9.57451	10.2581	11.0852	11.9616	11.0972	12.4619	10.7967	12.4556	11.0548	11.0641	11.5841
AMY	10.0929	10.3171	10.5353	11.1835	11.8406	12.3597	12.0573	12.2269	11.5935	12.0892	11.7317	11.6168	11.6307
CBC	10.4649	10.5863	10.241	10.796	10.6485	11.8153	11.72	12.0826	11.9787	12.3861	12.1763	11.894	12.1902
HIP	9.87324	10.3336	10.5053	10.796	11.6841	12.5634	11.9992	11.9209	11.3889	12.1796	11.4789	11.6155	11.7061
MD	9.81282	10.3776	10.6582	11.1591	11.7319	12.5391	12.228	12.5358	12.504	12.2241	11.8775	12.2617	12.324
STR	9.71967	9.61989	10.5751	11.1364	11.9717	12.353	11.9285	12.0714	12.0834	12.1085	11.7447	11.6634	11.7975

Supplementary table 19: Data matrix representing log2 transformed values of ***ATP1B3*** (encoding for Na-K ATPase β3) in different regions at different developmental periods. White cells represent samples where the gene is expressed, while gray cells represent samples considered not expressed (cutoff value of 5.5 was used to determine expression status).

Area	3	4	5	6	7	8	9	10	11	12	13	14	15
OFC	5.80051	6.00555	6.41394	5.6133	6.5186	5.95826	6.38852	5.75789	5.42606	6.00342	5.80569	5.45866	6.14254
MFC	6.03415	5.82103	6.7363	6.58925	6.75597	5.93856	6.14211	6.15511	5.09601	5.93705	6.10406	6.02026	5.96246
DFC	6.04035	5.85234	6.7723	6.11121	6.65345	5.76969	5.97799	6.10018	5.51696	5.40178	5.35113	5.53228	6.09774
VFC	5.85203	6.11297	6.92357	6.29437	6.75322	6.05137	5.77426	6.34526	5.79356	5.86784	5.60237	5.64525	6.18231
M1C	6.22082	5.83192	6.33597	6.01857	6.9742	5.33221	5.66643	5.84993	6.08116	5.56531	5.94492	5.4367	5.99866
S1C	6.30896	6.02188	6.54419	6.05588	6.89114	6.57803	5.90549	6.17838	5.75097	5.81166	6.04392	5.9839	6.26169
IPC	6.34817	6.04365	6.51848	6.63114	6.85283	5.79696	6.22069	6.17827	5.57847	5.69979	5.55954	5.86351	6.26899
STC	5.98219	6.02582	7.3234	6.81198	6.58526	6.84179	6.2249	6.12729	5.54925	5.81256	6.04823	5.97307	6.38609
A1C	6.08684	5.84761	6.9606	6.06379	6.77818	6.40161	6.32669	6.48199	5.37254	5.91534	6.05488	5.90482	6.45349
ITC	5.80017	5.846	6.25941	5.86197	6.62744	5.69482	6.24895	6.42329	5.6159	5.6493	5.98953	6.11272	6.26193
V1C	6.84466	6.46795	6.6639	7.0061	6.75501	6.25184	5.94994	6.64866	5.28415	6.08954	6.09084	5.62578	6.30355
AMY	6.16515	5.97426	6.52585	5.87108	6.53939	6.16339	5.12707	5.77209	5.66817	5.22466	6.19596	5.8179	6.01739
CBC	5.18833	5.50317	6.56113	5.65827	7.36451	7.09292	7.33683	8.23296	6.31395	6.47136	6.48209	7.47465	7.45683
HIP	5.91848	5.998	6.13431	6.09339	6.21225	6.37297	5.41238	5.78568	5.42328	5.76578	6.20828	5.69173	6.23234
MD	5.65723	5.46326	6.63517	6.60217	7.15598	5.35024	6.28009	6.54925	6.47824	6.04252	5.68579	6.15562	5.86414
STR	5.73456	5.87651	6.90592	6.79606	5.58483	6.57666	5.57384	6.37166	6.14436	6.42767	6.92091	6.48536	6.57116

Supplementary table 20: Data matrix representing log2 transformed values of ***ATP1B4*** (encoding for Na-K ATPase β4) in different regions at different developmental periods. White cells represent samples where the gene is expressed, while gray cells represent samples considered not expressed (cutoff value of 5.5 was used to determine expression status).

Area	3	4	5	6	7	8	9	10	11	12	13	14	15
OFC	3.74003	3.7434	3.71499	3.6376	3.75049	3.72472	3.74574	3.90315	3.78427	3.70949	3.73803	3.6466	3.71806
MFC	3.77205	3.75737	3.61085	3.65632	3.70337	3.73436	3.77688	3.88739	3.76264	3.74863	3.79172	3.78984	3.6781
DFC	3.76109	3.76415	3.66354	3.70858	3.64536	3.69148	3.75843	3.85887	3.86724	3.73106	3.75874	3.83041	3.70038
VFC	3.77262	3.69365	3.60918	3.66057	3.71793	3.77774	3.75401	3.70064	3.74816	3.72707	3.73871	3.77789	3.70331
M1C	3.72015	3.75615	3.69621	3.7727	3.78391	3.74673	3.76437	3.91047	3.89289	3.70845	3.71529	3.79272	3.70218
S1C	3.7386	3.83746	3.6264	3.63819	3.70831	3.8241	3.78759	3.77993	3.7159	3.77014	3.72216	3.68029	3.79682
IPC	3.77754	3.73461	3.6282	3.70393	3.74065	3.79019	3.91688	3.86934	3.76658	3.75125	3.72783	3.74766	3.75966
STC	3.74009	3.79557	3.68381	3.68997	3.68647	3.75657	3.75686	3.82681	3.78578	3.7042	3.66898	3.75473	3.759
A1C	3.75704	3.83678	3.6472	3.71043	3.78654	3.73959	3.85501	3.73549	3.78972	3.81216	3.72905	3.76498	3.7385
ITC	3.75158	3.79186	3.64751	3.71532	3.70237	3.74316	3.78847	3.81465	3.84365	3.73451	3.69708	3.78087	3.72511
V1C	3.68652	3.75304	3.59984	3.67302	3.98734	3.81833	3.73762	3.80449	3.8899	3.80784	3.64763	3.70386	3.90737
AMY	3.76666	3.65865	3.65624	3.68403	3.79499	3.78199	3.734	3.89851	3.81349	3.85456	3.75463	3.74239	3.89806
CBC	3.7185	3.69754	3.60108	3.70037	3.82095	3.71796	3.73839	3.68928	3.709	3.64562	3.74904	3.87408	3.79147
HIP	3.6576	3.69073	3.72308	3.68019	3.72827	3.82743	3.77899	3.71881	3.87146	3.7594	3.71071	3.85346	3.86855
MD	3.81047	3.7159	3.70693	3.68461	3.9167	3.96379	3.82548	3.58875	3.71484	3.72139	3.68642	3.72293	3.82846
STR	3.7736	3.74682	3.66413	3.66372	3.91917	3.68443	3.84316	3.84304	3.8189	3.74326	3.63552	3.70792	3.75308

Supplementary table 21: Data matrix representing log2 transformed values of ***SYP*** (encoding for synaptophysin) in different regions at different developmental periods. White cells represent samples where the gene is expressed, while gray cells represent samples considered not expressed (cutoff value of 5.5 was used to determine expression status).

Area	3	4	5	6	7	8	9	10	11	12	13	14	15
OFC	7.5755	7.61018	7.70192	8.29754	10.8426	11.6138	11.2109	10.9942	10.8495	11.0269	10.9777	10.4939	10.7259
MFC	7.78979	7.75656	7.89149	8.5876	11.0715	11.5153	11.2357	11.1104	10.9899	10.795	11.0068	10.353	10.8444
DFC	7.70799	7.65083	7.57055	8.22652	10.5674	11.3284	11.3714	11.2559	10.9301	10.8556	11.2015	10.194	10.7157
VFC	7.66797	7.5905	8.33899	8.68926	10.6135	11.4487	11.256	11.056	10.7636	10.8858	10.8817	10.5413	10.7027
M1C	7.96427	7.9315	8.14116	8.84777	11.2387	11.283	11.2071	11.3846	10.7275	10.8271	10.9603	10.3642	10.8267
S1C	7.86941	8.01658	8.02218	8.97142	11.1292	11.4251	10.9856	11.1985	10.6718	10.8579	10.8365	10.5957	10.8109
IPC	7.82329	7.95245	8.37055	8.71966	10.7016	11.2308	11.2487	11.4502	10.9878	10.9287	10.8288	10.6177	11.0091
STC	7.76276	7.86805	7.99316	8.35085	10.6261	11.2517	11.2469	11.5059	10.7803	10.9006	11.0249	10.5475	10.8507
A1C	7.7144	7.75419	8.16038	8.4601	10.5599	11.2867	11.5568	11.4093	10.8623	10.9387	10.75	10.3492	10.8274
ITC	7.51039	7.78569	8.0853	8.52175	10.6339	11.2918	11.3016	11.31	10.774	10.8411	10.9757	10.5937	11.0055
V1C	8.30968	8.29668	8.07472	8.08909	10.6413	11.1307	11.245	11.2969	10.707	10.9317	10.9781	10.7616	10.3051
AMY	7.27442	7.12929	7.73534	7.81325	10.2925	11.0577	10.9663	10.9332	10.5749	10.797	10.7826	10.3474	10.8208
CBC	7.59352	7.47088	8.67153	8.31307	9.10232	10.2814	9.90809	9.89017	9.37927	10.1247	10.5778	9.46112	9.74485
HIP	7.00313	7.10552	8.40099	9.31575	10.2792	11.0506	10.7243	10.8491	10.7833	10.8191	10.8556	10.6875	10.878
MD	8.57044	8.76038	9.64564	10.1933	11.0596	10.8835	11.0478	10.5464	10.9031	10.781	11.0476	10.8846	10.507
STR	7.53613	7.28121	8.50181	8.3117	6.93301	9.44707	9.35145	9.60049	8.78553	9.08911	9.3896	8.92049	9.15804

Supplementary table 22: Data matrix representing log2 transformed values of ***DLG*** (encoding for PSD-95) in different regions at different developmental periods. White cells represent samples where the gene is expressed, while gray cells represent samples considered not expressed (cutoff value of 5.5 was used to determine expression status).

Area	3	4	5	6	7	8	9	10	11	12	13	14	15
OFC	9.87702	9.82039	9.74601	9.62339	10.1304	10.6326	10.7508	10.4896	9.94122	10.625	10.4472	10.5112	10.3023
MFC	10.2713	10.035	9.55493	9.83635	9.6291	10.7629	10.8952	10.4154	10.3803	10.5102	10.6908	10.252	10.6866
DFC	10.1266	9.94422	9.51958	9.78965	10.0694	10.8154	10.7866	10.556	10.6202	10.7612	10.5149	10.7402	10.4885
VFC	9.84864	9.92176	9.40167	9.83534	10.1466	10.9199	10.8763	10.1266	10.2454	10.7374	10.3488	10.3186	10.135
M1C	10.1303	10.2022	9.98845	10.0188	10.042	10.8756	11.1282	10.598	10.4103	10.5515	10.4192	10.5629	10.1883
S1C	10.1802	10.0234	10.0166	9.93439	10.0656	10.5452	10.907	10.1145	10.6218	10.5729	10.4271	10.6445	10.0974
IPC	10.0186	10.038	9.87377	9.95349	9.93133	10.925	11.1163	10.204	10.3452	10.5636	10.6367	10.6185	10.2172
STC	10.043	10.0285	9.16774	9.60753	9.76262	10.8133	10.9044	10.5662	10.364	10.6781	10.3686	10.4361	10.1118
A1C	10.0151	9.80571	9.63379	9.66658	9.79791	10.8315	10.8833	10.4344	10.476	10.6587	10.3765	10.3224	10.1457
ITC	9.92903	9.95789	9.69268	9.60957	10.1046	11.0005	11.031	10.4031	10.6408	10.8003	10.5928	10.5922	9.97667
V1C	10.4467	10.3878	9.72915	9.69769	9.52537	10.883	10.9464	10.2626	10.221	10.4878	10.3155	10.1065	9.67507
AMY	9.76658	9.55075	9.26952	9.15762	9.16845	10.5508	10.4931	10.0247	10.2009	10.4223	10.1514	10.3926	10.0423
CBC	9.71696	9.79224	8.85514	9.11604	9.30273	9.9283	9.80618	9.83742	10.103	10.3198	10.2805	10.109	10.2655
HIP	9.59735	9.78292	9.66752	9.54255	9.10558	10.4957	10.6113	10.0854	10.2161	10.4478	10.2127	10.646	10.4189
MD	9.76502	10.0032	9.68372	9.50092	8.68588	10.6323	10.3823	9.89519	10.3998	10.2588	9.79977	9.53426	9.48009
STR	10.3273	9.83216	10.1075	9.78477	7.74497	10.4235	10.8963	10.609	11.5911	10.9014	10.4481	10.5311	10.6743

Supplementary table 23: Data matrix representing log2 transformed values of ***CAST*** (encoding for calpastatin) in different regions at different developmental periods. White cells represent samples where the gene is expressed, while gray cells represent samples considered not expressed (cutoff value of 5.5 was used to determine expression status).

Area	3	4	5	6	7	8	9	10	11	12	13	14	15
OFC	5.74053	5.63274	6.06237	5.65108	6.94823	7.07482	7.63212	8.31464	8.23316	8.36425	8.48855	8.4111	8.69943
MFC	5.17142	5.51882	5.94255	6.06033	7.44019	7.41997	7.64332	8.17485	8.32197	8.4194	8.45511	8.40415	8.43723
DFC	5.45619	5.38196	5.75039	5.52771	7.31307	7.19466	7.54747	8.15254	7.94675	8.56992	8.71432	8.2792	8.71587
VFC	5.59061	5.30953	5.78823	5.76558	6.98829	7.12339	7.82931	8.18177	8.17924	8.50576	8.62488	8.5083	8.70837
M1C	5.1817	4.94696	5.70844	6.20996	7.63702	7.67481	7.4338	8.30063	8.24072	8.76401	8.81716	8.54433	8.98324
S1C	5.11409	5.0669	5.78491	6.08732	7.20511	7.34918	7.49815	8.22571	8.23977	8.5253	8.65136	8.62512	8.78295
IPC	5.33142	5.14652	5.6251	5.78719	6.94682	7.13484	7.48906	8.09836	8.39355	8.4817	8.6171	8.36102	8.84213
STC	5.50867	5.17567	5.49577	5.49605	6.90446	7.04308	7.5711	7.63023	8.01701	8.40091	8.60063	8.29088	8.67641
A1C	5.4312	5.25355	5.0708	5.44266	6.88629	7.66737	7.45978	7.97217	8.08313	8.46055	8.62451	8.54243	8.87146
ITC	5.33343	5.13264	6.07425	5.6178	6.70705	6.94853	7.43926	7.76186	8.02929	8.27266	8.28475	8.00919	8.318
V1C	5.12673	5.20518	5.62942	5.73103	6.75611	7.25802	7.58477	7.9496	8.36782	8.30241	8.75848	8.81383	8.66904
AMY	5.79869	5.83637	5.92513	6.33908	7.47543	7.53495	7.4593	7.6638	7.98269	8.1933	8.17634	8.52123	8.22639
CBC	5.96013	6.00937	6.37943	6.59783	7.44187	6.9227	6.71348	7.22188	7.48566	7.94324	7.79456	7.4783	7.68466
HIP	6.86782	6.33571	6.74357	7.172	7.80954	7.98804	7.81618	8.35939	8.04806	8.32982	8.67805	8.00056	8.54065
MD	6.1307	5.80165	6.95031	7.49836	7.99381	8.13703	8.10044	8.63162	8.83625	8.64642	8.87579	8.72645	8.68057
STR	6.15953	6.05918	6.30638	6.3601	7.95668	7.90099	7.87162	8.4529	8.47137	8.35768	8.62827	8.49047	8.21956

Supplementary table 24: Data matrix representing log2 transformed values of ***CAPN1*** (encoding for calpain 1 large subunit)in different regions at different developmental periods. White cells represent samples where the gene is expressed, while gray cells represent samples considered not expressed (cutoff value of 5.5 was used to determine expression status).

Area	3	4	5	6	7	8	9	10	11	12	13	14	15
OFC	8.80621	8.75417	8.59564	8.95154	7.69589	8.01776	7.70949	6.95571	7.83768	8.02003	7.83309	7.68155	7.70423
MFC	9.01074	8.88486	8.48467	8.804	7.50699	7.90592	7.94565	7.58587	7.96468	7.9242	7.80093	7.55859	7.83766
DFC	8.77614	8.59005	8.48483	8.72512	7.9122	7.89185	7.59099	7.63043	7.99432	8.07869	7.95121	7.87265	8.04341
VFC	8.64724	8.58252	8.52926	8.8192	7.77402	8.11075	7.72214	7.49025	8.10805	8.12695	8.04224	8.1463	7.57336
M1C	8.71414	8.74351	8.53389	8.90929	7.48318	7.95419	7.75216	7.59279	8.21034	8.09039	8.23764	8.14722	8.29544
S1C	8.66533	8.58202	8.56547	8.83185	7.43805	7.87517	7.71251	7.5439	8.39682	8.25172	8.07918	8.32753	7.88317
IPC	8.36988	8.5535	8.42989	8.75362	7.38094	7.89599	7.80317	7.53127	7.75327	7.95375	8.205	7.99416	7.64178
STC	8.10865	7.94741	8.22628	8.63607	7.91437	7.9296	7.52934	7.46528	7.7868	7.95933	7.98516	7.76984	7.87497
A1C	8.22343	8.36543	8.41077	8.6226	7.82657	7.85988	7.42077	7.19078	7.94445	7.68519	8.04718	7.97627	7.68096
ITC	7.65253	7.98808	8.53518	8.76376	7.90227	8.09737	7.80617	7.50279	7.85289	7.99137	7.91972	7.48203	7.53527
V1C	8.58322	8.43703	8.17618	8.35573	7.36017	7.78378	7.77511	7.19879	8.30357	7.93261	7.96096	7.76742	7.60514
AMY	7.86376	8.00903	7.98179	8.34954	7.44476	7.75334	7.99624	7.35258	7.97999	7.65987	7.57645	7.47327	7.45562
CBC	8.70157	8.6051	8.35717	8.53546	8.18246	8.94806	8.4768	8.16932	8.36634	8.61008	8.37429	7.81741	8.11595
HIP	8.29345	8.33742	8.55567	8.42582	7.39225	7.68421	7.7934	7.46272	8.24863	7.88058	7.58383	7.7757	7.51196
MD	9.25852	9.50366	8.98476	8.74956	7.19519	8.55123	8.54955	8.29677	8.95265	8.26978	8.36489	8.25963	7.87508
STR	8.39734	8.31041	8.44011	8.00823	6.90608	7.68348	7.79573	7.37503	8.94896	7.96224	7.49669	7.63587	7.70139

Supplementary table 25: Data matrix representing log2 transformed values of ***CAPN2*** (encoding for calpain 2 large subunit) in different regions at different developmental periods. White cells represent samples where the gene is expressed, while gray cells represent samples considered not expressed (cutoff value of 5.5 was used to determine expression status).

Area	3	4	5	6	7	8	9	10	11	12	13	14	15
OFC	8.00893	7.81551	7.96956	7.7738	8.36856	8.35968	8.15064	8.62207	8.28394	8.54931	8.26754	8.45074	8.53703
MFC	7.70277	7.76117	8.20161	7.70258	7.96788	8.4313	7.95538	8.70941	8.20249	8.67326	8.08316	8.43966	8.62286
DFC	7.84812	7.77756	7.99442	7.72625	8.44829	8.19883	7.82782	8.58478	8.05211	8.19579	7.96073	8.20532	8.4695
VFC	7.80161	7.38623	8.02249	7.91146	8.43477	7.74442	7.78382	8.87721	8.22978	8.39636	8.06885	8.29357	8.49054
M1C	7.81856	7.54237	7.55543	7.76089	8.2564	8.4086	7.68544	8.62435	7.752	8.49494	8.29741	8.28711	8.6483
S1C	7.7678	7.65783	7.45913	7.65716	8.15001	8.04877	7.48486	8.70903	8.04632	8.30641	8.25161	8.33664	8.35199
IPC	7.3444	7.33608	7.86432	7.77446	8.1893	8.23136	7.2537	8.44247	8.23678	8.34442	8.17922	8.10365	8.65233
STC	7.67973	7.3717	8.00019	7.87435	8.1686	8.40082	7.87274	8.06046	7.93811	8.43445	8.17312	7.95956	8.47598
A1C	7.78331	7.5286	7.70349	7.92345	8.18934	8.40252	7.50422	8.39671	8.07569	8.48334	8.23	8.24688	8.436
ITC	7.61002	7.24631	7.94798	8.0411	8.23728	8.24245	7.62679	8.30548	8.36707	8.44045	8.16145	8.07004	8.50576
V1C	7.32983	7.04693	8.0046	8.01323	8.0006	8.33063	7.59679	8.3574	8.07605	8.18426	8.10675	8.33399	8.41474
AMY	8.21763	8.16698	8.52108	8.3902	8.35441	8.63272	8.09952	8.34398	8.44574	8.60629	8.48872	8.92161	8.52166
CBC	8.39097	8.20038	8.60079	8.62557	8.39233	9.17229	8.76864	8.88178	8.74019	8.93472	8.7921	8.79795	9.09173
HIP	7.97106	7.88204	8.22633	8.13537	8.92875	8.6348	8.33919	8.75962	8.35529	8.72498	8.45313	8.3436	8.47304
MD	8.06913	8.00027	8.45375	8.46299	8.41357	8.40303	8.56681	9.18447	9.07337	8.79034	8.98216	8.89861	8.88379
STR	8.02983	7.96095	8.36494	8.26868	9.05501	8.7981	8.12492	8.72441	8.90522	8.69781	8.81528	8.85753	8.6807

Supplementary table 26: Data matrix representing log2 transformed values of ***CAPNS1*** (encoding for calpain small subunit 1) in different regions at different developmental periods. White cells represent samples where the gene is expressed, while gray cells represent samples considered not expressed (cutoff value of 5.5 was used to determine expression status).

Area	3	4	5	6	7	8	9	10	11	12	13	14	15
OFC	10.5594	10.6519	11.0793	11.2353	10.6546	11.3179	11.0659	10.183	10.8594	11.5992	11.3902	11.3771	11.3448
MFC	10.7706	10.9277	11.2254	11.349	10.537	11.4274	11.1841	10.4953	11.0452	11.472	11.4885	11.2775	11.4959
DFC	10.6492	10.882	11.2128	11.1189	10.5729	11.3501	11.0698	10.7686	11.0728	11.7666	11.5897	11.5638	11.6098
VFC	10.717	10.7534	11.0164	11.185	10.5834	11.35	11.3622	10.6177	11.097	11.7347	11.5404	11.503	11.518
M1C	10.7016	10.7087	10.7518	11.2576	10.4406	11.3463	11.4556	10.817	11.1318	11.6206	11.6053	11.6736	11.465
S1C	10.6914	10.7679	10.6694	11.2122	10.2029	11.4667	11.0606	10.5871	11.1664	11.5379	11.4683	11.5738	11.3855
IPC	10.7131	10.6575	11.0751	11.1223	10.4246	11.3217	11.3246	10.5548	10.8844	11.5904	11.6189	11.5397	11.4286
STC	10.6445	10.8563	10.9843	11.0492	10.3688	11.3422	11.1245	10.67	10.9615	11.4042	11.5435	11.4841	11.3906
A1C	10.802	10.8348	11.0602	11.0021	10.2361	11.3222	11.1179	10.6714	11.122	11.5226	11.4507	11.3825	11.4066
ITC	10.4328	10.7944	10.765	10.9191	10.5258	11.3361	11.2519	10.4355	10.9869	11.5294	11.493	11.4147	11.3635
V1C	10.7574	10.9724	10.9742	10.9436	9.71449	11.4264	10.8419	10.4859	10.9391	11.4011	11.3522	11.1855	11.0567
AMY	10.7911	10.7774	10.6186	10.9827	10.4212	11.2261	11.2606	10.6464	11.0633	11.3745	11.3606	11.0643	11.0363
CBC	10.7785	10.9209	11.2933	11.1614	10.963	11.5022	10.8033	10.5108	10.7466	11.6147	11.2214	10.9499	10.891
HIP	11.0836	11.159	11.197	11.2249	10.3874	11.3292	11.1584	10.7445	11.0875	11.1167	11.4175	11.2465	11.349
MD	10.8057	11.3699	11.0692	10.9616	10.4309	11.5383	11.277	11.1245	11.1742	11.5784	11.2764	10.9633	11.1584
STR	10.468	10.5781	10.7203	10.5476	10.4905	11.0581	10.7307	10.874	11.4398	11.6296	11.1817	11.0766	11.2721